Evaluation of a Chemical Forecast Model Using Advanced Aircraft Measurements

by

Andrew J. Wentland

A Master's Thesis submitted in partial fulfillment of the requirements for the degree of

Master of Science

Department of Atmospheric and Oceanic Sciences

at the

University of Wisconsin – Madison

May 2015

Abstract

Chemical forecast models are numerical models that help scientists and policy makers understand the chemical makeup of the atmosphere. Chemical forecast model assessment is an important process in determining the strengths and weaknesses of forecast simulations that give key insights to air quality policy questions. This is often accomplished by utilizing a variety of surface and, more recently, satellite observations for assessment. Over the course of July and August 2014, NASA, NCAR, and the state of Colorado launched cooperating field campaigns, DISCOVER-AQ and FRAPPE, to assess the air quality of the Denver metropolitan area. These missions employed several aircraft to conduct *in situ* measurements in addition to a network of ground-based measurements across the Front Range. Using the measurements made over the course of the field campaigns, the chemistry and meteorology of a "rapid refresh" configuration of the WRF-Chem model that is run in real-time at NOAA was assessed. In addition, an extensive AirNow network of air quality ground monitoring sites and satellite retrievals from NASA's ozone monitoring instrument (OMI) aboard the Aura satellite were used for model comparison.

AirNow comparison of $PM_{2.5}$ showed a correlation of 0.39 with the model overpredicting PM by 2.35 $\mu g/m^3$. A similar comparison for ozone found a correlation of 0.65 and a high model bias of 8.7 ppbv between the model and ground observations. Aircraft to model assessment found meteorology, with the exception of water vapor mixing ratio was generally consistent. The model underpredicted water vapor mixing ratio leading to questions of the model's ability to accurately forecast convection and vertical mixing. Chemical assessment of the model included ozone, carbon monoxide, methane,

formaldehyde, and nitrogen dioxide that were then compared to aircraft *in situ* measurements. *In situ* ozone assessment, like the AirNow comparison, found generally good correlation and little bias between model and observations. The lack of anthropogenic emission sources for methane caused a model underprediction near the surface where there was significant enhancement observed. Background carbon monoxide was slightly overpredicted with underprediction occurring closer to the surface, most likely again from anthropogenic sources. In contrast, formaldehyde saw little model bias in the upper troposphere with a high model bias closer to the surface. Finally, a very significant high model bias in nitrogen dioxide was identified both by in-situ aircraft measurements and by OMI. Beyond general analytics of model performance, a two-day period of high-observed ozone was investigated. Despite the generally accurate modeling of ozone throughout the field campaigns, an underprediction of ozone during the case study time period was found. Likely culprits of ozone underprediction include coarse horizontal model resolution impeding the modeling of dynamics and the parameterization of the planetary boundary layer.

Acknowledgments

This work would not be possible without the indispensable contributions of many individuals. Foremost, I would like to thank my advisors Dr. R. Bradley Pierce and Prof. Tracey Holloway for their guidance throughout my education and research at UW-Madison. None of this would be possible without both of their continued efforts and unparalleled dedication to research and student support.

Further, I would like to thank members of Dr. Pierce's and Prof. Holloway's research teams with special thanks to Dr. Monica Harkey and Allen Lenzen. In addition, thanks are due to Dr. Georg Grell and Dr. Steven Peckham for use of their model in this evaluation along with Dr. Travis Knepp for EPA ceilometer data and Dr. Ed Eloranta for UW lidar data. Thanks are also owed to all the participants and collaborators of the DISCOVER-AQ and FRAPPE field campaigns who worked tireless hours to insure the success of the missions. Beyond the aforementioned individuals and groups, I would like to thank my additional thesis reader, Dr. Greg Tripoli. Finally, I would like to thank my parents, family, and friends for their support through the years. This work was also made possible through funding by the NASA Air Quality Applied Sciences Team.

Table of Contents

Chapter 1: Background

Introduction

The Front Range is one of the fastest growing megaregions in the United States with a 2010 population of 5.5 million that is expected to grow 87% to 10.2 million by 2050 (Regional Plan Association, 2010). The Front Range is often referred to as the populated area that extends past the eastern boundary of the Rocky Mountains centered on Denver, Colorado. Despite ongoing efforts to improve air quality, near-surface air pollution remains a problem throughout the Front Range (Caiazzo et al., 2013). In the summer of 2014, a NASA Earth Venture program, Deriving Information on Surface Conditions from Column and Vertically Resolved Observations Relevant to Air Quality, DISCOVER-AQ, coincided with the state of Colorado and NCAR's Front Range Air Pollution and Photochemistry Experiment, FRAPPE. These field campaigns sought to characterize air quality in the Front Range to a degree that had not yet been accomplished.

The Front Range is an especially important area for detailed air quality studies due to unique atmospheric dynamics and chemical emission sources. Complex atmospheric flow patterns are driven by the Rocky Mountains to the

west of the Front Range that allow the formation of distinctive dynamic features such as up and downslope flow, the Denver Cyclone, and the Denver Convergence Zone (Tripoli & Cotton, 1989; Szoke, 1991; Bossert & Cotton, 1994). These unique atmospheric features have a significant impact on near-surface air quality (Haagenson, 1979; Reddy, 1995; Neff, 1997). These flow regimes can transport air masses with poor air quality away from urban environments and into more pristine environments to the west. In addition to mesoscale dynamics, the Rocky Mountains help drive intrusions of intercontinental air masses, transporting relatively high concentrations of ozone to the surface (Stohl et al., 2000).

Beyond the intricacies of the governing atmospheric dynamics that control surface air pollution in the Front Range, an assortment of emission sources add an additional layer of complexity in characterizing and modeling air pollution in this region. Industry, power generation, and transportation are all dominant sources of pollution in the Front Range near metropolitan areas like Denver, Boulder, and Fort Collins (EPA, 2011). Agriculture and wildfires are both significant biogenic sources that contribute to the degradation of air quality in the region. In recent years, increases in regional and continental wildfires have contributed to decreased air quality in the area that are expected to further decrease air quality in the future (Val Martin et al., 2015). A more

recent emerging source of air pollution in the Front Range is the development of oil and natural gas production. Sizable increases in the oil and natural gas industry in the Front Range, with few investigative air quality studies, leave an open question of the quantitative impact the growing industry has on air quality (Montzka et al., n.d.).

This work analyzes how well the rapid refresh configuration of the Weather Research and Forecasting model coupled with chemistry (WRF-Chem) ware able to accurately forecast the meteorology and atmospheric chemistry in the Front Range during the DISCOVER-AQ and FRAPPE field campaigns. Utilizing a variety of measurements from ground, research towers, aircrafts, and satellite observations, model performance was analyzed in the context of a number of questions including:

1. How well does the model predict near-ground and tropospheric pollution concentrations?
2. What role do dynamic features in the Front Range play in air quality?
3. How does the boundary layer behave and how does it influence the mixing of pollutants?

Answering these questions and conducting model assessment is important to air quality management in the Front Range in addition to improving modeling accuracy.

Front Range Meteorology

The Front Range climate is semi-arid with unpredictable weather due to the surrounding topography of the Rocky Mountains (Hansen, 1978). Summer in the Front Range is characterized by clear, warm mornings with clouds moving in from over the mountains in the afternoon that can often be accompanied by thunderstorms. The mountainous topography around the Front Range allows for unique dynamic and thermodynamic circulations to occur. It has been found that mountains have a substantial influence over the atmospheric conditions of regions around them even on clear days with uneventful synoptic conditions (Wolyn and McKee, 1993; Baumann et al., 1997). Characteristic circulation flows of the Front Range include anabatic and katabatic flow, the Denver Convergence Zone, and the Denver Cyclone.

Anabatic and katabatic winds, more commonly referred to as a mountain and valley breeze, are atmospheric flows that are driven by temperature gradients over mountainous topography common during the summers in the

Front Range (Christopherson, 1992; Baumann et al., 1997). Where anabatic winds are upslope flows driven by warm surface conditions relative to the atmosphere, katabatic winds are downslope flows driven by cool surface conditions relative to the atmosphere. In the Front Range, anabatic flow is commonly observed in the afternoon and early evening when the surface has warmed through solar insolation. Katabatic winds are often observed in the late evenings and early mornings in the Front Range when the slopes of the Rockies have cooled. Beyond the thermodynamic mechanism that forms upslope and downslope flow, certain synoptic conditions can also drive the atmospheric flow. High pressure north of the Front Range, low pressure South of the Front Range, and low pressure west of the Front Range can all enhance upslope flow (Hansen, 1978; Wolyn & Mckee, 1994). These upslope and downslope flows are important when studying air pollution in the Front Range as they are significant drivers of chemical transport and dispersion throughout the area.

The Denver Convergence-Vorticity Zone (DCVZ) is an area of convergence in the Front Range that can occur when a strong southeasterly wind is present in the region (Szoke & Brady, 1989; Wesley & Pielke, 1990). As this wind moves towards the foothills and Rocky Mountains, it is redirected towards the west and meets the usually geostrophic flow moving over the Rockies. The DCVZ represents the meeting of these atmospheric flows. While

research on the DCVZ is limited with regard to its effect of atmospheric chemistry, it is expected to enhance pollution concentrations near the convergence zone. It is important to note that the DCVZ is often confused with the Denver Cyclone. To further clarify, DCVZ is an area of convergence and shear while the Denver Cyclone is a mesoscale, stationary gyre.

The Denver Cyclone, like the DCVZ, develops due to the terrain of the Front Range and surrounding mountains. Unlike the DCVZ, the Denver cyclone is a mesoscale gyre whose spatial scale is on the order or 10km to 100km in diameter and can persist for up to 10 hours (Wilczak & Glendening, 1988; Szoke, 1991). The DCVZ and Denver Cyclone are commonly associated with each other due to similar flow regimes needed in generating each but neither is required for the other to develop. The cyclone develops in the boundary layer due to baroclinic conditions interacting with stress divergence profile over sloping topography. This in turn creates convergence and a gyre. While the cyclone has not been studied heavily in regard to atmospheric chemistry, it is hypothesized that the gyre should create higher local concentrations of pollutants within its circulation.

Front Range Air Chemistry

The variety of emission sources in the Front Range along with emissions that are transported into the region give its atmosphere a complex chemical makeup. Common primary pollutants observed, or pollutants emitted directly into the atmosphere, include carbon monoxide (CO), nitrogen oxides (NO_x) (Figure 1.2), volatile organic carbons (VOCs) such as formaldehyde (HCHO), and particulate matter (PM). The most common secondary pollutant, or chemical formed through chemical process in the atmosphere, is ozone (O_3) (Benedict et al., 2013; Brown et al., 2013; Dutton, Rajagopalan, Vedal, & Hannigan, 2010; Haagenson, 1979).

The National Ambient Air Quality Standards (NAAQS), established under the Clean Air Act, set federal standards of allowable concentrations of primary and secondary pollutants for counties in the United States. In the Front Range, a number of counties are in marginal non-attainment of the NAAQS 8-hour averaged ozone concentration (Figure 1.1). Ozone standards are both primary and secondary so that they ensure the protection of both sensitive groups and general human health. Non-attainment of O_3 in the Front Range is an ongoing motivation for continued air quality studies in the region including both the DISCOVER-AQ and FRAPPE field campaigns.

Both primary and secondary pollutants are significant concerns as they contribute to degradation of human health and loss of agricultural productivity. Generally, air pollution by nature affects the respiratory systems of humans and animals, but can also cause cardiac problems, cancer, and hematological problems. Of the common pollutants in the Front Range, ozone and particulate matter are harmful to agriculture causing reduced growth and death in plants either directly or indirectly by changing the pH of the growing medium (Seinfeld and Pandis, 2012).

Air pollutants observed in the Front Range come from a variety of anthropogenic and biogenic sources (NEI, 2011). The common primary pollutant, carbon monoxide, is a colorless and odorless gas produced when incomplete combustion of organic substances occurs. Common sources of carbon monoxide in the Front Range include motor vehicles and wildfires. Nitrogen oxides, like carbon monoxide, form when nitrogen and oxygen interact during combustion with sources including motor vehicles, industrial sources, and biogenic sources like lightning and fertilizer (Figure 2.3). Formaldehyde is a highly reactive gas at room temperature that is a byproduct of volatile organic compounds oxidizing (Seinfeld and Pandis, 2012). Volatile organic compounds are produced from natural sources such as forest fires and

from anthropogenic combustion processes in power plants and from fuel combustion in vehicles.

One primary pollutant that is not found in a gaseous phase is particulate matter. Particulate matter is not a single chemical molecule but rather a mixture of varying particles of different sizes and compositions. It is categorized by physical size with PM_{10} representing particles less than 10 microns in diameter and $PM_{2.5}$ representing particles less than 2.5 microns in diameter. PM_{10} is commonly found emitting from fugitive sources like unpaved roads and heavy construction areas, whereas $PM_{2.5}$ can be found as a product of both biogenic and anthropogenic combustion (Seinfeld and Pandis, 2012).

Secondary pollutants are not directly emitted from sources but rather form in the atmosphere through chemical process such as photochemical reactions (Jacob, 1999). These reactions occur when primary pollutants react with each other and often with radiant energy like ultraviolet radiation. The most common form of secondary pollution is photochemical smog that is made up of volatile organic compounds, nitrogen oxides, and ozone. The large majority of ozone found in the troposphere is not directly emitted but rather forms when carbon monoxide, volatile organic compounds, and nitrogen oxides react in the presence of ultraviolet light. Correspondingly, nitrogen dioxide

(NO_2) is formed in the atmosphere when nitrogen oxide (NO) reacts with ozone or other free radicals.

To gain insight into air pollution in the Front Range, Chapter 2 will present the methods used to conduct a model to observational comparison of July and August 2014 during the FRAPPE and DISCOVER-AQ Field Campaigns. Chapter 3 will highlight general findings of the comparison, while Chapter 4 will analyze a specific case study of high-observed ozone and model performance. Finally, concluding remarks will be presented in Chapter 5.

Chapter 1 Figures

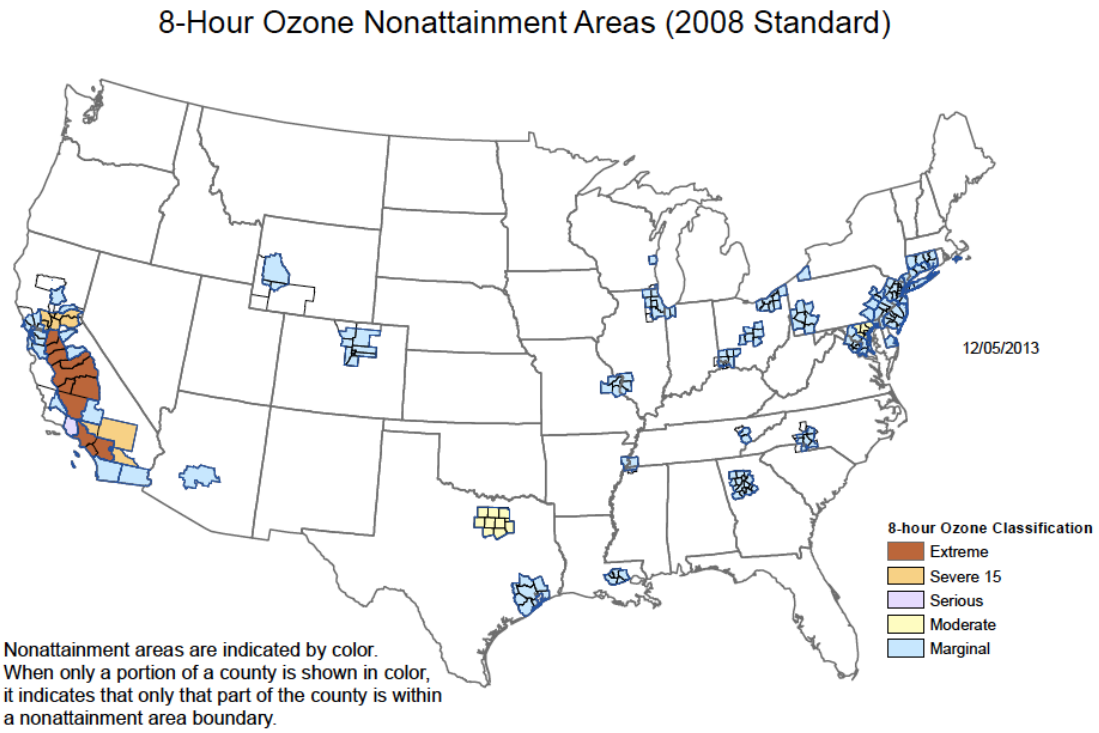

Figure 1.1: US Counties in non-attainment of EPA NAAQS ozone. *Source: EPA, 2013*

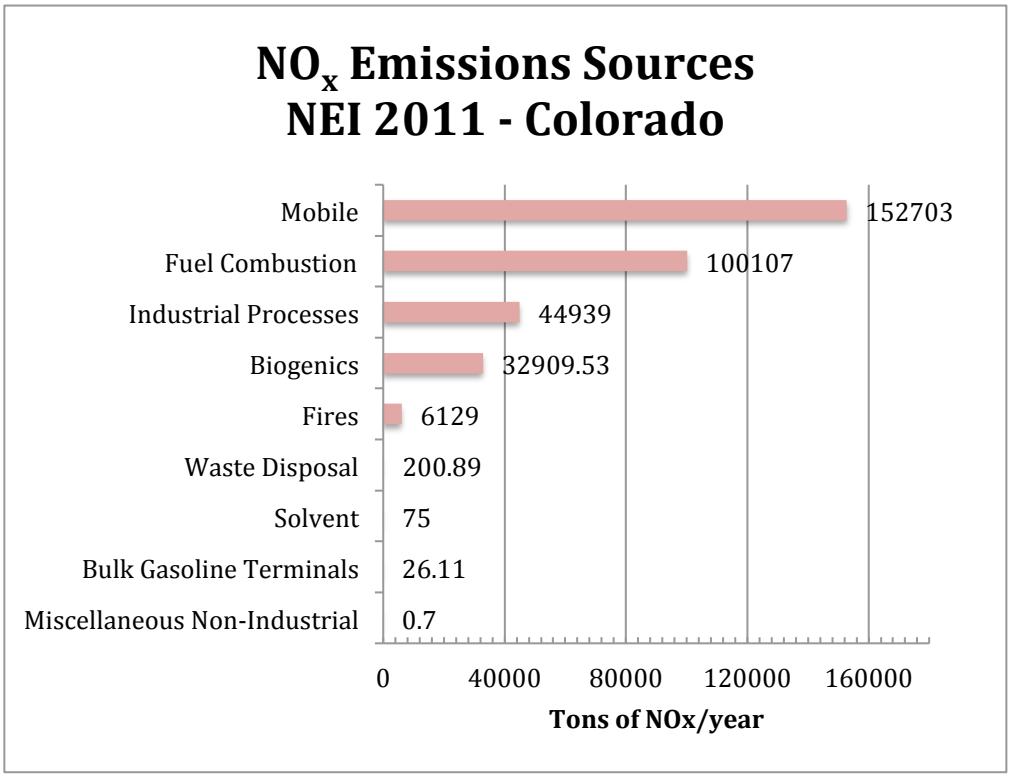

Figure 1.2: NEI 2011 NOx inventory for Colorado by sector. *Source: NEI 2011*

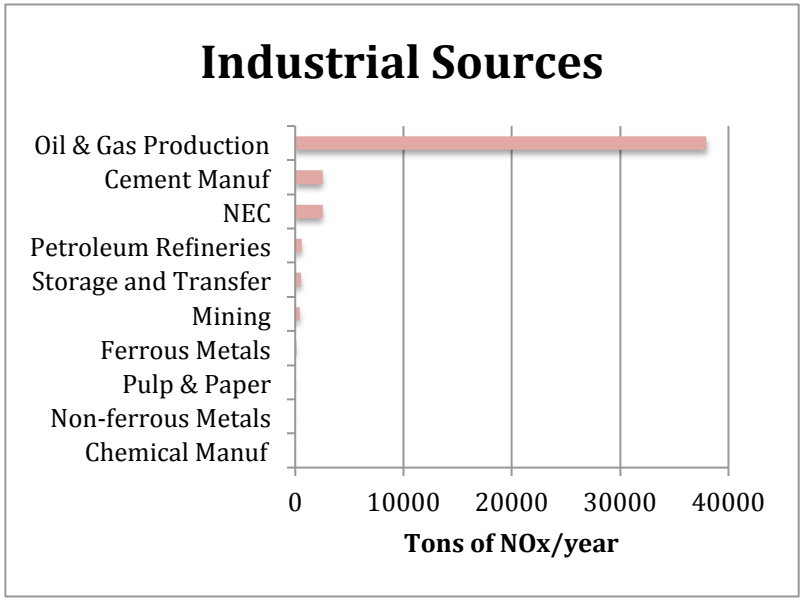

Figure 1.3: NEI 2011 NOx inventory for Colorado Industrial Sources. *Source: NEI 2011*

Chapter 1 References

Baumann, K., Williams, E. J., Olson, J. a., Harder, J. W., & Fehsenfeld, F. C. (1997). Meteorological characteristics and spatial extent of upslope events during the 1993 Tropospheric OH Photochemistry Experiment. Journal of Geophysical Research, 102, 6199. doi:10.1029/96JD03251

Benedict, K. B., Day, D., Schwandner, F. M., Kreidenweis, S. M., Schichtel, B., Malm, W. C., & Collett, J. L. (2013). Observations of atmospheric reactive nitrogen species in Rocky Mountain National Park and across northern Colorado. Atmospheric Environment, 64, 66–76. doi:10.1016/j.atmosenv.2012.08.066

Bossert, J. E., & Cotton, W. R. (1994). Regional-Scale Flows in Mountainous Terrain. Part II: Simplified Numerical Experiments. Mon. Weather Rev. Retrieved from http://www.ncbi.nlm.nih.gov/entrez/query.fcgi?db=pubmed&cmd=Retrieve&dopt=AbstractPlus&list_uids=A1994NU46600005

Brown, S. S., Thornton, J. a., Keene, W. C., Pszenny, A. a P., Sive, B. C., Dubé, W. P., … Wolfe, D. E. (2013). Nitrogen, Aerosol Composition, and Halogens on a Tall Tower (NACHTT): Overview of a wintertime air chemistry field study in the front range urban corridor of Colorado. Journal of Geophysical Research: Atmospheres, 118, 8067–8085. doi:10.1002/jgrd.50537

Caiazzo, F., Ashok, A., Waitz, I. a., Yim, S. H. L., & Barrett, S. R. H. (2013). Air pollution and early deaths in the United States. Part I: Quantifying the impact of major sectors in 2005. Atmospheric Environment, 79, 198–208. doi:10.1016/j.atmosenv.2013.05.081

Christopherson, Robert W. (1992). Geosystems: An Introduction to Physical Geography. Macmillan Publishing Company. p. 155. ISBN 0-02-322443-6.

Dutton, S. J., Rajagopalan, B., Vedal, S., & Hannigan, M. P. (2010). Temporal patterns in daily measurements of inorganic and organic speciated PM2.5 in Denver. Atmospheric Environment, 44(7), 987–998. doi:10.1016/j.atmosenv.2009.06.006

EPA. (2013). 2011 National Emissions Inventory, Version 1 Technical Support Document, (November).

Haagenson, P. (1979). Meteorological and climatological factors affecting Denver air quality. Atmospheric Environment (1967), 13(1977), 79–85. Retrieved from http://www.sciencedirect.com/science/article/pii/0004698179902476

Hansen, W. R., Chronic, J., & Matelock, J. (1978). Climatography of the Front Range Urban Corridor and vicinity, Colorado. A graphical summary of climatic conditions in a region of varied physiography and rapid urbanization.Professional Papers-US Geological Survey (USA).

Jacob, D. (1999). Introduction to atmospheric chemistry. Princeton University Press.

Montzka, A., Sweeney, C., Andrews, A., & Dlugokencky, M. (n.d.). Estimation of Emissions from Oil and Natural Gas Operations in Northeastern Colorado. Epa.Gov, 2010–2013. Retrieved from http://www.epa.gov/ttnchie1/conference/ei20/session6/gpetron.pdf

Neff, W. D. (1997). The Denver Brown Cloud Studies from the Perspective of Model Assessment Needs and the Role of Meteorology. Journal of the Air & Waste Management Association, 47(January 2015), 269–285. doi:10.1080/10473289.1997.10464447

Reddy, P. J. (1995). Development of a statistical model for forecasting episodes of visibility degradation in the Denver metropolitan area. Journal of Applied …, 34. Retrieved from http://journals.ametsoc.org/doi/abs/10.1175/1520-0450(1995)034%3C0616%3ADOASMF%3E2.0.CO%3B2

Regional Plan Association (2015). America 2015: Megaregions: The Front Range. http://www.america2050.org/front_range.html

Seinfeld, J. H., & Pandis, S. N. (2012). Atmospheric chemistry and physics: from air pollution to climate change. John Wiley & Sons.

Stohl, a., Spichtinger-Rakowsky, N., Bonasoni, P., Feldmann, H., Memmesheimer, M., Scheel, H. E., … Mandl, M. (2000). The influence of stratospheric intrusions on alpine ozone concentrations. Atmospheric Environment, 34(9), 1323–1354. doi:10.1016/S1352-2310(99)00320-9

Szoke, E. J. (1991). Eye of the Denver Cyclone. Monthly Weather Review. doi:10.1175/1520-0493(1991)119<1283:EOTDC>2.0.CO;2

Szoke, E. J., & Brady, R. H. (1989). Forecasting Implications of the 26 July 1985 Northeastern Colorado Tornadic Thunderstorm Case. Monthly Weather Review. doi:10.1175/15200493(1989)117<1834:FIOTJN>2.0.CO;2

Tripoli, G. J., & Cotton, W. R. (1989). Numerical Study of an observed Orogenic Mesoscale Convective Systems. Part I: Simulated Genesis and Comparison with Observations. Monthly Weather Review.

Val Martin, M., Heald, C. L., Lamarque, J.-F., Tilmes, S., Emmons, L. K., & Schichtel, B. A. (2015). How emissions, climate, and land use change will impact mid-century air quality over the United States: a focus on effects at national parks. Atmospheric Chemistry and Physics, 15(5), 2805–2823. doi:10.5194/acp-15-2805-2015

Wesley, D. A., & Pielke, R. A. (1990). Observations of blocking-induced convergence zones and effects on precipitation in complex terrain. Atmospheric Research. doi:10.1016/0169-8095(90)90014-4

Wilczak, J. M., & Glendening, J. W. (1988). Observations and mixed-layer modeling of a terrain-induced mesoscale gyre: The Denver cyclone. Monthly Weather Review, 116. Retrieved from http://journals.ametsoc.org/doi/abs/10.1175/1520-0493(1988)116%3C2688%3AOAMLMO%3E2.0.CO%3B2

Wolyn, P. G., & Mckee, T. B. (1994). The Mountain-Plains Circulation East of a 2-km-High North–South Barrier. Monthly Weather Review. doi:10.1175/1520-0493(1994)122<1490:TMPCEO>2.0.CO;2

Chapter 2: Methods

The forecast model analyzed in this study was the research version of the Rapid Refresh with Chemistry model (RR-Chem). The model is a rapid refresh configuration of the Weather Research and Forecasting model coupled with chemistry (WRF-Chem) run at NOAA/ESRL (Grell et al., 2005; Koch et al., 2000). A number of observational data sets from ground observations, research tower observatories, *in situ* aircraft observations, and satellite retrievals were used to assess the RR-Chem model. Ground observations were obtained through the AirNow air quality network and the Boulder Atmospheric Observatory research facility. Aerial observations were included from the DISCOVER-AQ field campaign using NASA's P3B research aircraft along with data from the FRAPPE field campaign obtained through NSF and NCAR's C-130 research aircraft. Satellite observations were obtained through NASA's Ozone Monitoring Instrument (OMI) aboard the Aura Satellite. Statistical analysis was conducted using the aforementioned observational data sets to assess model performance in the Front Range for the duration of the DISCOVER-AQ and FRAPPE field campaigns.

RR-Chem Model Overview

In this study, the RR-Chem model was used to forecast and quantify meteorology and air chemistry. Meteorological model performance was conducted on potential temperature, wind speed, and water vapor mixing ratio, as they all are important in the governance of atmospheric chemistry (Jacob, 1999; Seinfeld and Pandis, 2012). The model's chemical performance was analyzed in terms of carbon monoxide, nitrogen dioxide, formaldehyde, particulate matter, and ozone, as they are all predominate chemical species found in the area and are detrimental to human health (EPA, 2012; Lave and Seskin, 2013).

The RR-Chem model's meteorology is generated through the Weather Research and Forecasting model (WRF) (Grell et al., 2005). The WRF model is a 3-dimensional numerical weather prediction and atmospheric simulation that is a nonhydrostatic and compressible model (Grell et al., 2012; Skamarock et al., 2008). The model is used by a variety of operational forecasting and atmospheric research groups. The model resolution analyzed in this study has a 13.5 km by 13.5 km horizontal resolution and 51 vertical layers based on hydrostatic pressure coordinates. Meteorological output used included horizontal and vertical velocity components, perturbation potential temperature, perturbation geopotential, and perturbation surface pressure of dry air. Model

output was generated every 3 hours with initialization occurring every 12 hours at 00:00 UTC and 12:00 UTC.

Several WRF physics options were used in this model simulation. The microphysics scheme used was the WRF single–moment 3–class and 5–class schemes that have been found to improve the ice cloud-radiation feedback that drives high-cloud physics, surface precipitation, and average temperature over previous configurations (S.Y. Hong & Dudhia, 2004). The planetary boundary layer (PBL) physics scheme used was the Yonsei University Scheme. This PBL scheme has been found to improve vertical diffusion in the boundary layer with more accurate prediction of convective inhibition (Hong et al., 2006). Cumulus parameterization was based on Grell–Freitas Ensemble Scheme that is commonly used in high-resolution mesoscale models not unlike the RR-Chem model. This parameterization allows for interactions with aerosols simulating more realistic precipitation and increases of water and ice in cloud tops (G. Grell & Freitas, 2014). Longwave and shortwave radiation schemes were based on RRTMG Shortwave and Longwave Schemes that have been found to produce more accurate radiative forcing results when long lived greenhouse gasses, ozone, and water vapor are included in the simulation (Iacono et al., 2008).

The 2011 National Emissions Inventory (NEI) provided sectored emissions sources for the RR-Chem model (EPA, 2013). Pollutants included in the inventory are those that comprise the National Ambient Air Quality Standards (NAAQS) in addition to Hazardous Air Pollutants (HAPs) detailed in the Clean Air Act (Kuykendal, 2005). Emissions sources include point sources, nonpoint sources, on-road sources, non-road sources, and event sources. Event sources include significant anthropogenic and natural burning such as structure fires and wildfires. Point sources relevant to the Front Range that have been updated in the 2011 inventory to include industrial processes such as oil and gas production (VOCs, CO, NO_x), biomass burning (CO, VOCs), and agricultural burning ($PM_{2.5}$, SO_2, CO, NO_x, VOCs).

Biogenic emissions were provided through the Model of Emissions of Gases and Aerosols from Nature (MEGAN) (Guenther et al., 2012). Lateral boundary conditions for the model used 1-degree resolved conditions from the Real-time Air Quality Modeling System (RAQMS) (Pierce, et al., 2007). The RR-Chem model forecasts also included chemical deposition, photolysis, and convective and turbulent chemical transport with the later calculated concurrently with WRF (Fast et al., 2006).

The atmospheric chemical mechanism used in the model is based on Version 2 of the Regional Acid Deposition Model (Chang et al., 1989; Stockwell et al., 1990). The primary use of the Regional Acid Deposition Model is for gas phase reactions in atmospheric chemistry models. Aerosol parameterization, both primary and secondary, is based on the Modal Aerosol Dynamics Model for Europe (Ackermann et al., 1998).

Observational Data

Model validation of surface conditions was conducted using a number of observational data sets including the AirNow air quality network and the Boulder Atmospheric Observatory research facility. The AirNow air quality network uses federal reference monitoring techniques in line with state standards for air quality monitoring (Hawley, 2007). The network consists for over 2,000 monitoring stations in over 300 cities that provide real time pollution concentrations (Dye, AIRNow Program (U.S.), & Sonoma Technology Inc, 2003). Hourly data was used from monitoring stations throughout the Front Range and the continental US (CONUS) to assess the accuracy of the model in forecasting $PM_{2.5}$ and O_3 near-surface concentrations on an hourly basis.

The Boulder Atmospheric Observatory research facility, located in Erie, Colorado, was used to analyze boundary layer conditions up to 300 meters through use of the on-site tower (BAO Tower). Meteorological conditions in addition to ozone concentrations at the ground, 100 m, 200 m, and 300 m were used in model evaluation. BAO Tower was of particular interest in this study as it was a tower site that was incorporated in the DISCOVER-AQ's P3-B regular flight plan. In supplement of BAO Tower, the Environmental Protection Agency's ceilometer and the University of Wisconsin – Madison's High Spectral Resolution (HSRL) LIDAR were used to monitor the planetary boundary layer growth (Eloranta, 2005).

DISCOVER-AQ aircraft measurements were made using NASA's P3-B that had a maximum flight time of 14 hours and followed circuit pattern to investigate temporal variation in atmospheric composition (Figure 2.1) (NASA, 2014). FRAPPE aircraft measurements were made using the NSF/NCAR C-130 that was able to fly for up to 10 hours with a 2,900-mile range (UCAR/NCAR - Earth Observing Laboratory, 1994). The C-130's flight plans were designed as exploratory missions to investigate spatial variations in atmospheric composition. Most all measurements from the C-130 were made within the boundary layer. Airborne chemical measurements of CO, NO_2, HCHO, O_3, and CH_4 in addition to meteorological measurements of potential temperature,

humidity, and wind speed were used for model evaluation. Ozone and nitrogen oxides were observed with a chemiluminescence instrument (Ray et al., 2009). Formaldehyde was measured with an Aerolaser AL50, while carbon monoxide was measured using a compact atmospheric multispecies spectrometer (Bukowiecki, 2002; Li, Parchatka, Königstedt, & Fischer, 2012). Methane observations were made using the Picarro instrument (Rella, 2010).

Satellite measurements of NO_2 were made using the Ozone Measurement Instrument (OMI) aboard the Aura Satellite (Ahmad et al., 2003). Satellite overpasses occurred once daily in the early to mid afternoon when pollution levels were typically highest. Measurements of NO_2 were made of the total tropospheric atmospheric nitrogen dioxide column value. To insure optimal satellite data, no observations were included when the cloud fraction was above 30% and data quality flags were applied when interpolating and gridding satellite retrievals to remove erroneous data. Satellite retrievals were taken with a resolution of 13km x 24km at nadir and a 2600km swath width (Levelt et al., 2006). Measurements were then interpolated and regridded to RR-Chem's 13km x 13km horizontal spatial grid for statistical evaluation to the model.

Chapter 2 Figures

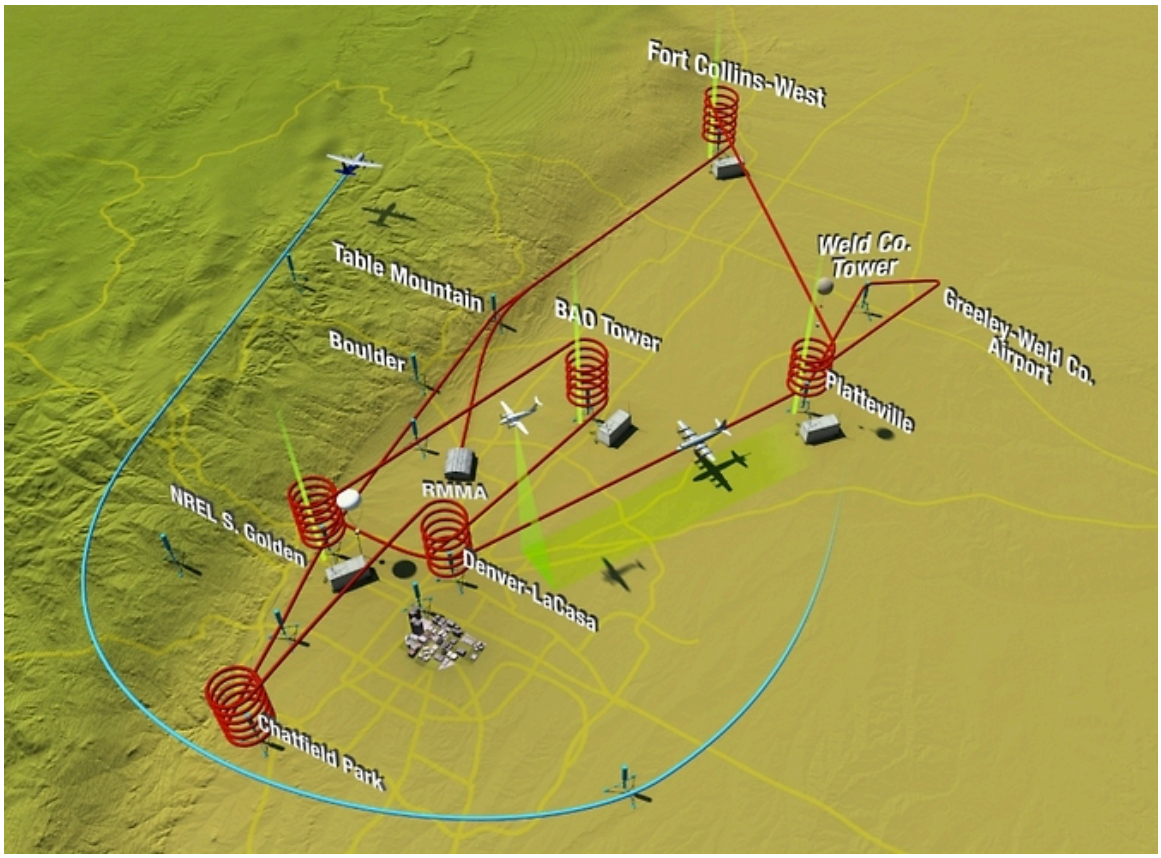

Figure 2.1: NASA's P3B flight track for DISCOVER-AQ 2014.

Source: NASA, 2014

Chapter 2 References

Ackermann, I.J., Hass, H., Memmesheimer, M., Ebel, A., Binkowski, F.S., Shankar, U., 1998. Modal aerosol dynamics model for Europe: development and first applications. Atmospheric Environment 32 (17), 2981–2999.

Ahmad, S. P., Levelt, P. F., Bhartia, P. K., Hilsenrath, E., Leppelmeier, G. W., & Johnson, J. E. (2003). Atmospheric products from the ozone monitoring instrument (OMI). Society of Photo-Optical Instrumentation Engineers (SPIE) Conference Series, 5151(2), 619–630. doi:10.1117/12.506042

Bukowiecki, N., Dommen, J., Prevot, A. S. H., Richter, R., Weingartner, E., & Baltensperger, U. (2002). A mobile pollutant measurement laboratory—measuring gas phase and aerosol ambient concentrations with high spatial and temporal resolution. Atmospheric Environment, 36(36), 5569-5579.

Chang, J.S., Binkowski, F.S., Seaman, N.L., McHenry, J.N., Samson, P.J., Stockwell, W.R., Walcek, C.J., Madronich, S., Middleton, P.B., Pleim, J.E., Lansford, H.H., 1989. The regional acid deposition model and engineering model. State-of-Science/Technology, Report 4, National Acid Precipitation Assessment Program, Washington, DC.

Dye, T. S., AIRNow Program (U.S.), & Sonoma Technology Inc. (2003). Guidelines for Developing an Air Quality (ozone and PM2.5) Forecasting Program, 1.

Eloranta, E. E. (2005). High spectral resolution lidar (pp. 143-163). Springer New York.

EPA, (2013). 2011 National Emissions Inventory, Version 1 Technical Support Document, (November).

Fast, J. D., Gustafson, W. I., Easter, R. C., Zaveri, R. a., Barnard, J. C., Chapman, E. G., … Peckham, S. E. (2006). Evolution of ozone, particulates, and aerosol direct radiative forcing in the vicinity of Houston using a fully coupled meteorology-chemistry-aerosol model. Journal of Geophysical Research: Atmospheres, 111(21), 1–29. doi:10.1029/2005JD006721

Grell, G., McKeen, S., Barth, M., Pfister, G., Wiedinmyer, C., Fast, J. D., ... & Freitas, S. (2012). WRF/Chem Version 3.3 User's Guide. US Department of Commerce, National Oceanic and Atmospheric Administration, Oceanic and Atmospheric Research Laboratories, Global Systems Division.

Grell, G. a., Peckham, S. E., Schmitz, R., McKeen, S. a., Frost, G., Skamarock, W. C., & Eder, B. (2005). Fully coupled "online" chemistry within the WRF model. Atmospheric Environment, 39(37), 6957–6975. doi:10.1016/j.atmosenv.2005.04.027

Grell, G., & Freitas, S. R. (2014). A scale and aerosol aware stochastic convective parameterization for weather and air quality modeling. Atmospheric Chemistry and Physics, 14(10), 5233–5250. doi:10.5194/acp-14-5233-2014

Guenther, a. B., Jiang, X., Heald, C. L., Sakulyanontvittaya, T., Duhl, T., Emmons, L. K., & Wang, X. (2012). The model of emissions of gases and aerosols from nature version 2.1 (MEGAN2.1): An extended and updated framework for modeling biogenic emissions. Geoscientific Model Development, 5(6), 1471–1492. doi:10.5194/gmd-5-1471-2012

Hawley, K. (2007). Federal Register, 72(53), 81–95.

Hong, S. Y., & Dudhia, J. (2004). Testing of a new nonlocal boundary layer vertical diffusion scheme in numerical weather prediction applications. Bulletin of the American Meteorological Society, 2(1), 2213–2218.

Hong, S.-Y., Noh, Y., & Dudhia, J. (2006). A New Vertical Diffusion Package with an Explicit Treatment of Entrainment Processes. Monthly Weather Review, 134(9), 2318–2341. doi:10.1175/MWR3199.1

Iacono, M. J., Delamere, J. S., Mlawer, E. J., Shephard, M. W., Clough, S. a., & Collins, W. D. (2008). Radiative forcing by long-lived greenhouse gases: Calculations with the AER radiative transfer models. Journal of Geophysical Research: Atmospheres, 113(13), 1–8. doi:10.1029/2008JD009944

Jacob, D. (1999). Introduction to atmospheric chemistry. Princeton University Press.

Koch, S. E., Benjamin, S. G., Mcginley, J. a, Brown, J. M., Schultz, P., Szoke, E. J., … Grell, G. (2000). Real-Time Applications of the Wrf Model At the Forecast Systems Laboratory, 1–6.

Kuykendal, W. (2005). Emissions inventory guidance for implementation of ozone and particulate matter national ambient air quality standards (NAAQS) and regional haze regulations. DIANE Publishing.

Lave, L. B., & Seskin, E. P. (2013). Air pollution and human health. Routledge.

Levelt, P. F., Hilsenrath, E., Leppelmeier, G. W., Van Den Oord, G. H. J., Bhartia, P. K., Tamminen, J., … Veefkind, J. P. (2006). Science objectives of the ozone monitoring instrument. IEEE Transactions on Geoscience and Remote Sensing, 44(5), 1199–1207. doi:10.1109/TGRS.2006.872336

Li, J., Parchatka, U., Königstedt, R., & Fischer, H. (2012). Real-time measurements of atmospheric CO using a continuous-wave room temperature quantum cascade laser based spectrometer. Optics Express, 20(7), 7590. doi:10.1364/OE.20.007590

NASA, (2014). NASA P-3B Airborne Science Laboratory. http://www.nasa.gov/pdf/541828main_P-3BFactSheet.pdf

Pierce, R. B., et al. 2007: Chemical data assimilation estimates of continental U.S. ozone and nitrogen budgets during the Intercontinental Chemical Transport Experiment–North America, J. Geophys. Res., 112, D12S21, doi:10.1029/2006JD007722.Ray, J. D., Stedman, D. H., & Wendel, G. J. (1986). Fast chemiluminescent method for measurement of ambient ozone. *Analytical Chemistry*, *58*(3), 598-600.

Rella, C. (2010). Accurate Greenhouse Gas Measurements in Humid Gas Streams Using the Picarro G1301 Carbon Dioxide / Methane / Water Vapor Gas Analyzer Experimental Determination of the Water Vapor Correction for the G1301. Water.

Seinfeld, J. H., & Pandis, S. N. (2012). Atmospheric chemistry and physics: from air pollution to climate change. John Wiley & Sons.

Skamarock, W. C., Klemp, J. B., Dudhi, J., Gill, D. O., Barker, D. M., Duda, M. G., … Powers, J. G. (2008). A Description of the Advanced Research WRF Version 3. Technical Report, (June), 113. doi:10.5065/D6DZ069T

Stockwell, W.R., Middleton, P., Chang, J.S., Tang, X., 1990. The second-generation regional acid deposition model chemical mechanism for regional air quality modeling. Journal of Geophysical Research 95, 16343–16367.

UCAR/NCAR - Earth Observing Laboratory, (1994). NSF/NCAR Hercules C130 Aircraft. http://dx.doi.org/10.5065/D6WM1BG0

Chapter 3: Model Evaluation

Introduction

Model evaluation is an important process in determining the strengths and deficiencies of chemical forecasting simulations that give key insights to air quality policy questions. Due to the complicated nature of atmospheric chemical modeling, meteorological and chemical evaluations are both needed due to the interdependent nature of meteorology and air chemistry. Ideally, each model grid box would be analyzed continuously but due to limited resources, a mixture of ground observations, aircraft *in situ* measurements, and satellite observations are used to holistically assess the model. Ground observations monitor near surface atmospheric conditions, while aircraft and satellite observations deliver observations of the vertical distribution and column concentrations of atmospheric pollutants.

Ground stations provide near surface pollution measurements that help scientists understand the impact of air pollution on populations and crops. Aircraft measurements allow one to gain a vertically resolved understanding of how well the model performs throughout the troposphere. While ground stations and aircraft measurements are convenient, they are often spatially limited, so satellite measurements allow for more all-inclusive spatial

assessment. Like ground and aircraft observations, satellite comparisons also come with negative tradeoffs. Ambiguity in air mass weighting factors can blur the truth of satellite retrievals, and lack of vertical resolution hampers model assessment at otherwise discretized levels throughout the atmosphere.

In the comparison, we utilize the AirNow network both in the CONUS in addition to the network in Colorado. Aircraft measurements from both NASA's P3B and NCAR's C130 allow for vertically resolved meteorological and chemical assessment of the model. Finally, NASA's ozone monitoring unit aboard the Aura Satellite is used to observe column nitrogen dioxide levels for CONUS and Colorado.

Ground Observation Comparison

Model to ground-level chemical analysis was performed with a series statistical metrics and observational data sets. The AirNow Network provided hourly ozone (O_3) and particulate matter ($PM_{2.5}$) measurements that were compared with model output at the same locations (Dye et al., 2003). AirNow sites are more often located near urban environments so assessment is more indicative of modeling accuracy, or lack thereof, of populated regions (Figure 3.1; Figure 3.2). For our evaluation, the majority of AirNow sites were located

in and around the Denver Metropolitan Area, home of the DISCOVER-AQ and FRAPPE Field Campaigns.

Continental United States AirNow Results

Ground level ozone in CONUS was in general agreement with model simulations with a correlation of 0.65, a bias of -8.69 ppb, and a root mean square error of 16.21 ppb when concentrations under 120 ppb were analyzed (Figure 3.5). Concentrations of ozone above 120 ppb were not used in statistical analysis due to the likelihood of observational errors. Similarly, $PM_{2.5}$ measurements under 100 $\mu g/m^3$ were analyzed across CONUS with a lower correlation than ozone, 0.39 (Figure 3.3). Despite a lower correlation between model and observations, the mean bias of -2.34 μg/m3, and the root mean square error of 9.4 μg/m3 were smaller than what was found for ozone.

Colorado AirNow Results

For the interior of Colorado, ozone was modeled with a correlation of 0.66, similar to CONUS (Figure 3.6). Model bias was substantially improved relative to the overall performance in the CONUS domain with a mean bias of -0.21 ppb and a root mean squared error of 12.82 ppb. Particulate matter less

than 2.5 microns in Colorado held the weakest correlation of 0.19 (Figure 3.4). However, mean bias and root mean squared error for $PM_{2.5}$ were improved compared to CONUS with values of -0.71 $\mu g/m^3$ and 5.7 $\mu g/m^3$ respectively.

AirNow Discussion

In terms of ozone, model accuracy was similar to past studies using WRF-Chem at a model resolution of 12 km that found correlations in the range of 0.6 to 0.7 but generally better than other atmospheric chemistry models (McKeen et al., 2007; Simon, Baker, & Phillips, 2012; Žabkar et al., 2015). Despite the promising findings, it is important to question if the model's performance for a secondary pollutant like ozone is correct for the right reasons or the wrong reasons. Due to the nonlinear relation between volatile organic compounds and nitrogen oxides, the primary ingredients of tropospheric ozone, overestimation of nitrogen oxides can lower ozone significantly in certain regimes (Jacob, 1999).

$PM_{2.5}$ performed with a slightly less degree of accuracy compared with previous studies (McKeen et al., 2007; Saide et al., 2011; Simon et al., 2012). Variations in past studies' gas phase mechanism and configuration result in varying modeling results of particulate matter (Zhang, Chen, Sarwar, & Schere,

2012). Greater exploration into other chemical mechanisms may be a viable path for improvement of $PM_{2.5}$ in the RR-Chem simulation. In addition, variations in particulate matter emissions compounded by the complex terrain have proven to be difficult to model and aerosols during the field campaigns were lower than what is generally expected in the Front Range (Saide et al., 2011).

Aircraft *in situ* Comparison

NASA's P3B and NCAR's C130 were utilized in our model assessment to vertically resolve the atmosphere for chemical and meteorological variables. In terms of meteorology, potential temperature, wind speed, and water vapor mixing ratio were used to assess the model's atmospheric stability and horizontal and vertical mixing. Chemically, ozone, methane, carbon monoxide, formaldehyde, and nitrogen dioxide were analyzed to gain a greater understanding for some of the more predominate air pollutants in the Front Range (EPA, 2013). Flights for the P3B and C130 were made nearly everyday, sometimes twice daily, for the entirety of the field campaigns. In addition to vertically discretized measurements, median column amounts were also calculated for the five chemical species.

Potential Temperature

Potential temperature, a common measure of atmospheric static stability, was measured throughout the atmosphere by both the P3B and C130 (Figure 3.7; Figure 3.8). Generally, the RR-Chem model accurately predicted potential temperature below 500mb. Above 500mb, there was slight underprediction but varying sample size limited the number of observations in that pressure regime. C130 observations showed an inversion commonly occurring below 800mb that the model did not predict. This discrepancy could indicate an improperly modeled boundary layer or near surface inversions. If an inversion is not accounted for in the model, pollutant concentrations may be underestimated due to greater vertical mixing as inversions typically limit mixing height thus increasing near surface concentrations (Marshall and Plumb, 1965).

Wind Speed

The horizontal mixing of pollutants and the subsequent concentration of pollutants is primarily controlled by the wind, highlighting the importance in the accurate modeling of wind speed and direction (Ying, Tie, & Li, 2009). For both *in situ* observational datasets, modeled wind speed was underpredicted throughout the entire atmosphere (Figure 3.9; Figure 3.10). P3B observations

were typically 4 m/s greater than the modeled wind speed. While a low model bias was present, correlation was generally good throughout the atmosphere for the P3B comparison. Like temperature, P3B observations were limited so the resulting difference is likely enhanced due to a limited sample size.

C130 *in situ* observations and RR-Chem performance were similar to the P3B comparison in that modeled wind speed was generally under predicted while past studies have found both over and underestimation of wind speed by similar model configurations (Tuccella et al., 2012; Yerramilli et al., 2010). However, correlation was not as accurate with the model predicting a localized wind speed maximum near 700mb. The underprediction of wind speed may cause several modeled inaccuracies including higher modeled concentrations of pollutants due to decreased mixing and less downstream concentrations from point sources.

Water Vapor Mixing Ratio

Water vapor mixing ratio can be related to vertical mixing ability of the atmosphere, convective available potential energy (CAPE), in addition to the likelihood of precipitation (Marshall and Plumb, 1965). Model and P3B comparison showed a low model bias that was more significant below 700mb

(Figure 3.11). The model, on average, underpredicted the mixing ratio by approximately 1g/kg below the 700mb pressure level whereas above, the model underprediction was less significant with only an average difference of a few tenths of a gram per kilogram. Similar to other the meteorological observations, lacks of measurements above 500mb were likely to blame for the statistical variations at these altitudes.

C130 and model comparison was similar to the P3B below 700mb with model underprediction of water vapor while above the 700mb level, the model slightly overpredicted water vapor, in contrast to the consistent under prediction by the model with regard to the P3B flight track (Figure 3.12). Similar underprediction of water vapor and relative humidity has previously been documented (Fast et al., 2006; Yerramilli et al., 2010). Underprediction by the model for both *in situ* datasets would most likely result in the model to underestimate convection and precipitation and thus less vertical mixing and wet deposition in the chemical predictions.

Ozone

Ozone was generally well predicted for both the P3B and C130 modeled flight track (Figure 3.13; Figure 3.14). P3B *in situ* measurements below 700mb

showed a slightly low model bias but were still well correlated. Above 700mb, the RR-Chem model showed no significant bias when compared to *in situ* P3B measurements. The average P3B column measurement was approximately $30 \cdot 10^{15}$ mol/cm^2, 1.1 DU, greater than the RR-Chem model with the median situ column amount of $584 \cdot 10^{15}$ mol/cm^2, 21.7 DU, and a modeled column amount of $552 \cdot 10^{15}$ mol/cm^2, 20.5 DU.

C130 *in situ* measurements were slightly less correlated with a greater overall bias compared to the model. While little model bias occurred below 800mb, slight overprediction of approximately 10ppbv ozone arose between 750mb and 550mb. In contrast from the P3B observations and model track, RR-Chem had a slightly higher median column amount of $573 \cdot 10^{15}$ mol/cm^2, 21.3 DU, compared to the median *in situ* column of $549 \cdot 10^{15}$ mol/cm^2, 20.4 DU. While either aircraft observed little model bias, ozone is not directly emitted into the atmosphere. Instead, ozone concentrations are governed by precursors like volatile organic compounds, nitrogen oxides, and carbon monoxide, in addition to atmospheric conditions. Like the findings for the AirNow analysis, further investigation into those factors is needed to determine if ozone production is accurate due to correct emissions estimates and model physics or due to incorrect modeling (Georg a. Grell et al., 2005; Yerramilli et al., 2010).

Methane

In addition to ozone and its precursors, methane emissions in the Front Range are an ongoing problem. For the *in situ* analysis of methane, an adjustment was applied to background methane levels since the RAQMS boundary conditions were fixed at 1990 levels (EPA, 2013). In the upper troposphere above 700mb, both the C130 and P3B accurately captured methane (Figure 3.15; Figure 3.16). Both airplanes observed significant enhancement of methane below 700mb that the model failed to capture. The P3B observed the highest methane measurements between the two aircraft with readings as high as 2800 ppbv, well above the model peak predictions at the same pressure level of approximately 1850 ppbv. Closest to the surface, *in situ* observations, even at their lowest measurements, were still higher than model prediction.

The model's low bias may be attributed to decision not to use anthropogenic emissions in this particular configuration of RR-Chem. Despite this, median column amounts for both aircraft when averaged throughout the entire atmosphere were satisfactory with the P3B and RR-Chem median column amounts of $17.3 \bullet 10^{18}$ mol/cm^2 and $17.2 \bullet 10^{18}$ mol/cm^2, respectively. Similarly, the C130, that observed less variation of methane compared to the model near the surface, had a median column measurement of $17.4 \bullet 10^{18}$ mol/cm^2 compared to the model's column measurement of $17.4 \bullet 10^{18}$ mol/cm^2.

The closer agreement between the C130 and model track could possibly be attributed to the aircraft flying over more rural and mountainous areas where anthropogenic emissions are not as common. The greater variation in methane in the upper troposphere observed by the C130 compared to the P3B could also be explained through upslope flow carrying methane into the more mountainous regions where the C130 flew. It is difficult to compare methane to previous studies without the inclusion of point sources, as it should be a priority to include those inventories in updates to the model.

Carbon Monoxide

Carbon monoxide, typically a pollutant resulting from combustion within automobiles, was modeled and observed throughout the Front Range with relatively good accuracy (Figure 3.17; Figure 3.18). The P3B and RR-Chem model mapped to the P3B flight track observed a relative peak in carbon monoxide around 800mb with higher concentrations being observed generally closer to the surface. Less model variance and the most accurate model results came above 600mb. Nearest to the surface, significant spikes in carbon monoxide concentrations were observed that were not captured by RR-Chem. Overall, the model over predicted the median column amount by approximately

$90 \cdot 10^{15}$ mol/cm^2 with the model predicting $993 \cdot 10^{15}$ mol/cm^2 and the P3B *in situ* instrument observing $905 \cdot 10^{15}$ mol/cm^2.

While the median column difference between C130 *in situ* measurements and the modeled flight track was smaller with column amounts of $934 \cdot 10^{15}$ mol/cm^2 and $964 \cdot 10^{15}$ mol/cm^2 respectively, the model did not capture significant surface enhancement that was observed. While the model was unable to capture near surface enhancement, it performed well compared to previous studies evaluating carbon monoxide (Tie et al., 2007).

Formaldehyde

Formaldehyde, a common tracer of volatile organic compounds was also observed by both the P3B and C130 (Figure 3.19; Figure 3.20). Unlike methane, near surface enhancement of HCHO was over predicted by the model. In both *in situ* observational datasets, a peak in HCHO occurs near 800mb to 850mb with lower observations near the surface. Generally above 800mb, HCHO in-situ was well correlated with the RR-Chem model. The P3B flight track in particular had the greatest difference to the model near the surface with a median RR-Chem column of $10.5 \cdot 10^{15}$ mol/cm^2 compared with an *in situ* measurement of $8.4 \cdot 10^{15}$ mol/cm^2. The C130 median column was $9.7 \cdot 10^{15}$

mol/cm^2 compared with an RR-Chem median column value of $10.1 \bullet 10^{15}$ mol/cm^2. This is in contrast to previous studies that have found an underestimation of HCHO using WRF-Chem and CMAQ and is most likely an issue with the NEI 2011 emissions inventory (Barth et al., 2014; Czader, Li, & Rappenglueck, 2013).

Nitrogen Dioxide

Nitrogen dioxide measurements aboard both aircrafts found substantial overestimation by the model through most of the troposphere (Figure 3.21; Figure 3.22). P3B observations show the most significant overestimation of NO_2 is found below 600mb where RR-Chem over predicted concentrations by approximately 2-3 times the amount observed. Above 600mb, the P3b show most consistent but varying observations when compared to the model. The model median column was about 3 times higher than the *in situ* observations with respective column amounts of $8.4 \bullet 10^{15}$ mol/cm^2 and $3.0 \bullet 10^{15}$ mol/cm^2.

C130 *in situ* measurements also pointed towards a high bias by the model from approximately 550mb to the surface. Above 550mb unexplained high measurements were reported by the C130, well above model results. The origin of these anomalously high measurements remains unresolved. Due to the high

measurements, the *in situ* median column value is greater than the model with a value of $9.5 \bullet 10^{15}$ mol/cm^2 compared to the RR-Chem model's median column value of $6.3 \bullet 10^{15}$ mol/cm^2. Despite the high-observed values by the C130, modeled NO_2 is overestimated by the model below 600mb.

Several recent studies have also found modeled overestimations of NO_x and have pointed at incorrect mobile emissions as a possible source of the error (Anderson et al., 2014; Ghude et al., 2013; Valin, Russell, Hudman, & Cohen, 2011). Nonlinear dependence of nitrogen oxides, VOCs, and ozone production imply that since NO_2 is incorrect, ozone concentrations that were being modeled with generally good agreement to observations may in fact be correctly modeled for the wrong reasons in urban environments. To further evaluate RR-Chem's NO_2 modeling, we employ NASA's ozone monitoring instrument to evaluate tropospheric nitrogen dioxide column values.

Aura Satellite Comparison

The Ozone Monitoring Instrument (OMI) aboard NASA's Aura satellite was used to calculate the NO_2 column over Colorado and the continental United States (Figure 3.23). Model output for NO_2, generated every 3 hours, was used at 21 UTC since that generally aligned with the average OMI overpass time for Colorado that most often occurred between 19 and 23 UTC. RR-Chem NO_2 was

vertically integrated for the troposphere and binned to the model's 13.5km horizontal resolution using the nearest neighbor algorithm. The top of the troposphere was calculated based on the World Meteorological Organizations standard for lapse rate in the tropopause, 2K/km (McCalla, 1981). Based on observations made by the satellite, areas where the cloud radiance fraction was greater than 30% were not included in statistical calculations of model performance of NO_2 tropospheric column.

Colorado OMI Comparison

OMI observations of Colorado and the Front Range show a regional maximum of approximately $4 \cdot 10^{15}$ mol/cm^2 centered on the Denver metropolitan area. Due to the persistence of clouds over the Rocky Mountains, a significant area could not be calculated due to cloud contamination. RR-Chem modeled NO_2 column values were spatially similar with a regional maximum over the Denver metropolitan area, but the model was nearly 3 times higher than observed values at $10 \cdot 10^{15}$ mol/cm^2. Beyond urban areas, background nitrogen dioxide column values are more closely aligned to modeled concentrations. Statistically, the correlation between model and observations is 0.38 with a high model bias of $0.69 \cdot 10^{15}$ mol/cm^2 and a root mean squared error

of $1.89 \bullet 10^{15}$ mol/cm^2 (Figure 3.24). Typically, the model shows a high bias at observational maxima and minima.

Continental United States OMI Comparison

Observations of the Ozone Monitoring Instrument were also compared to modeled values for the continental United States. Like Colorado, modeled NO_2 over the United States was greater than observed column values over most metropolitan areas. The most significant overestimation was observed in the Western United States, especially in the major cities of California like Los Angeles, San Francisco, and Sacramento. In rural areas, there was good agreement, relative to urban areas, with slight underestimation in very rural areas. Model to observation correlation for the continental United States was just under what was calculated for Colorado with a correlation coefficient of 0.35 and high model bias of $0.52 \bullet 10^{15}$ mol/cm^2 and root mean squared error of $2.10 \bullet 10^{15}$ mol/cm^2 (Figure 3.23). Like Colorado, the model simulated a high bias compared to the observational dataset. Beyond the continental United States, the RR-Chem model also significantly overpredicted NO_2 around the Calgary, Canada metropolitan area and surrounding regions.

OMI Discussion

Similar to the *in situ* findings, nitrogen dioxide is overestimated by approximately the same amount throughout not only Colorado but also the United States. Similar findings, while not to the extent of ours, have found problems with the emissions inventories and modeling of nitrogen oxides (Anderson et al., 2014; Ghude et al., 2013; Valin et al., 2011). One major difference is that this study only used tropospheric column amounts without applying an air mass factor, potentially biasing results.

Model Performance Discussion

The evaluation of the modeling of meteorology and chemistry by the RR-Chem model presented a mix bag of strengths and weaknesses of the model. Potential temperature was a relatively strong suit of the model with very little difference between simulation and aircraft observations. Chemically, ozone and carbon monoxide also performed well in model to observation analysis. Similarly, background methane concentrations performed well but anthropogenic enhancement near the surface was not included in this model simulation so it was not captured. Water vapor mixing ratio was slightly underpredicted by the model, which possibly contributed to problems in

capturing convection and mixing in the atmosphere. Formaldehyde and nitrogen dioxide were both overestimated by the model with overestimation of formaldehyde occurring near surface and nitrogen dioxide throughout the entire tropospheric column. These are likely problems not with the RR-Chem model itself but instead with the NEI 2011 emissions inventory.

Chapter 3 Figures

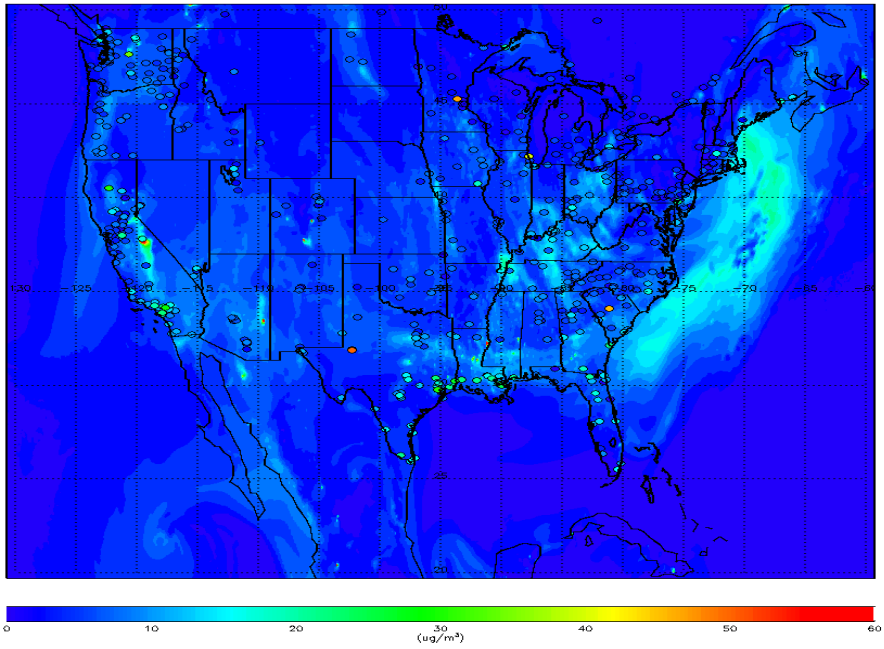

Figure 3.1: AirNow Network with modeled RR-Chem $PM_{2.5}$
July 28th, 2014

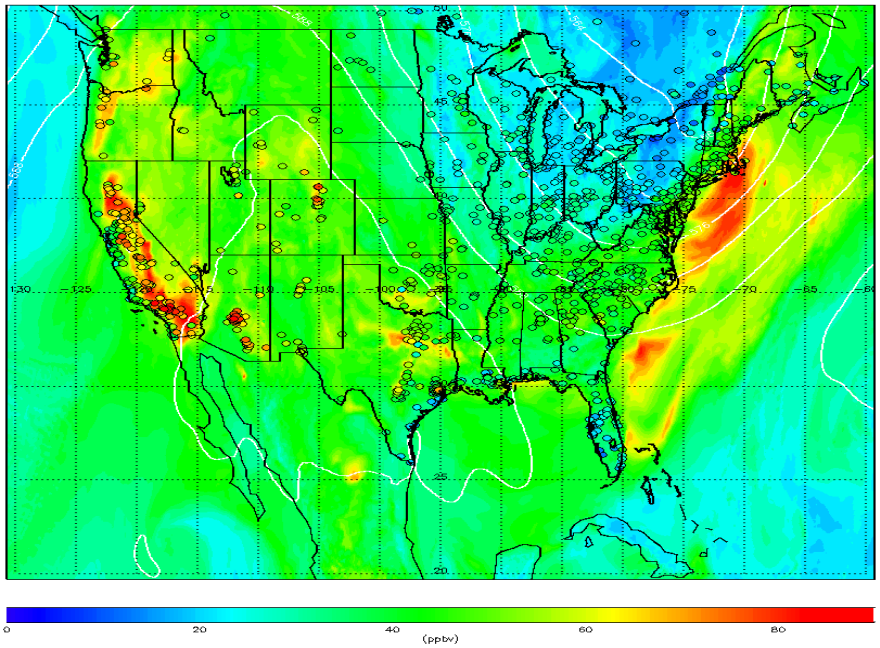

Figure 3.2: AirNow Network with modeled RR-Chem O_3
July 28th, 2014

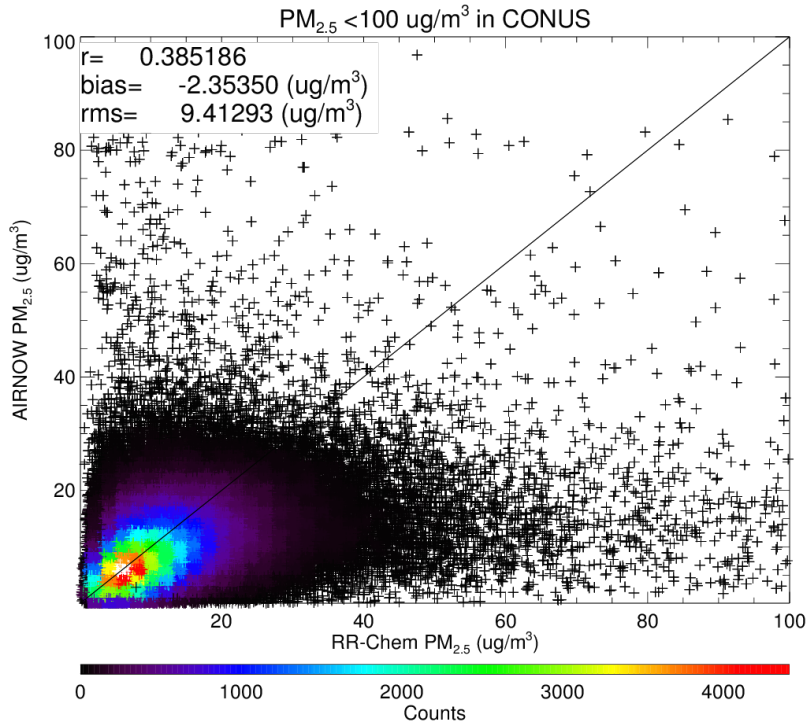

Figure 3.3: AirNow Network vs. RR-Chem $PM_{2.5}$ statistics in the United States

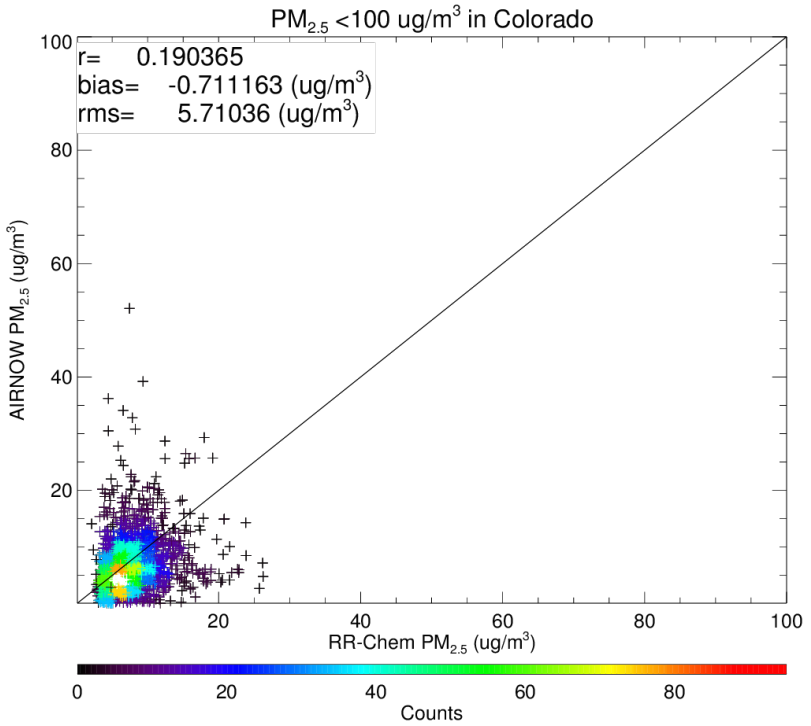

Figure 3.4: AirNow Network vs. RR-Chem $PM_{2.5}$ statistics in Colorado

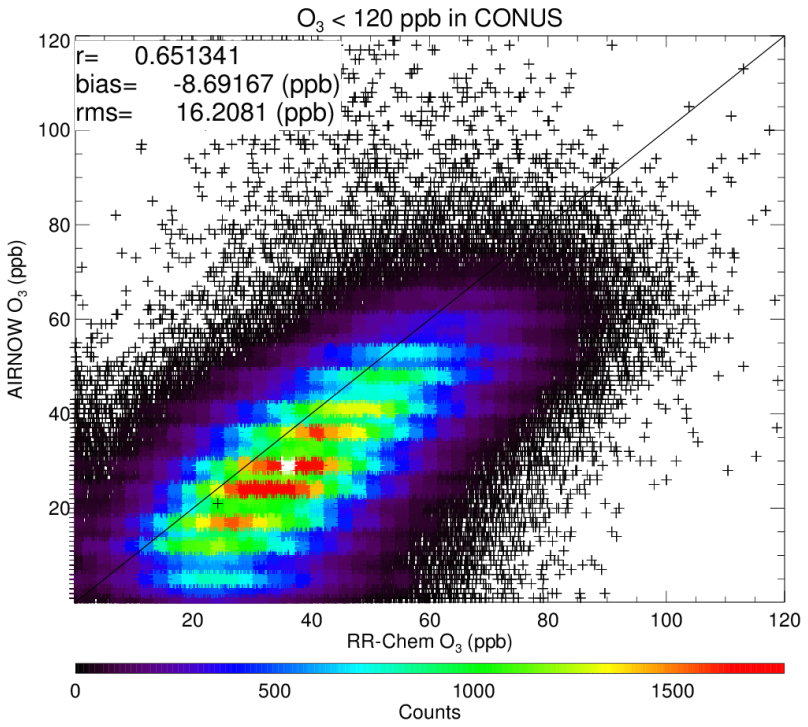

Figure 3.5: AirNow Network vs. RR-Chem O_3 statistics in the United States

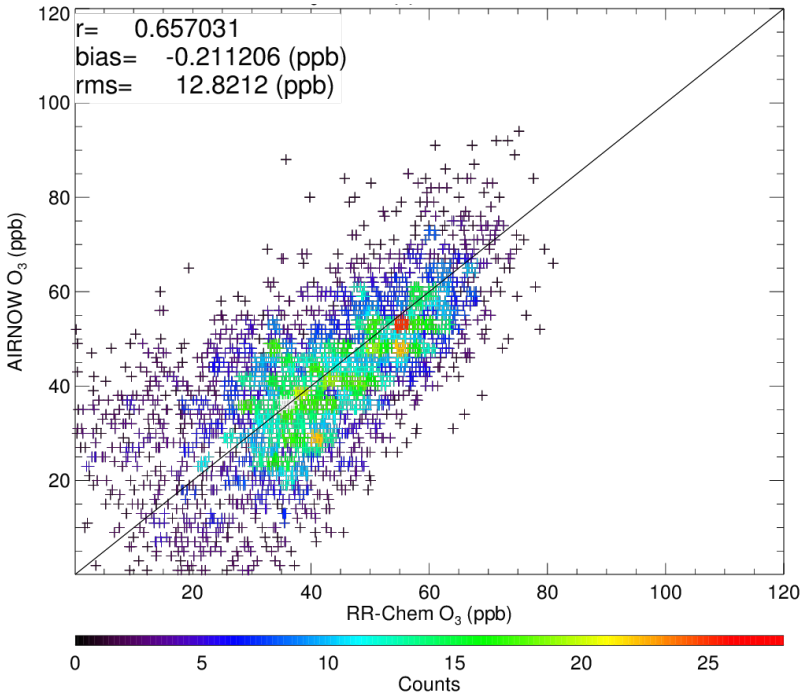

Figure 3.6: AirNow Network vs. RR-Chem O_3 statistics in Colorado

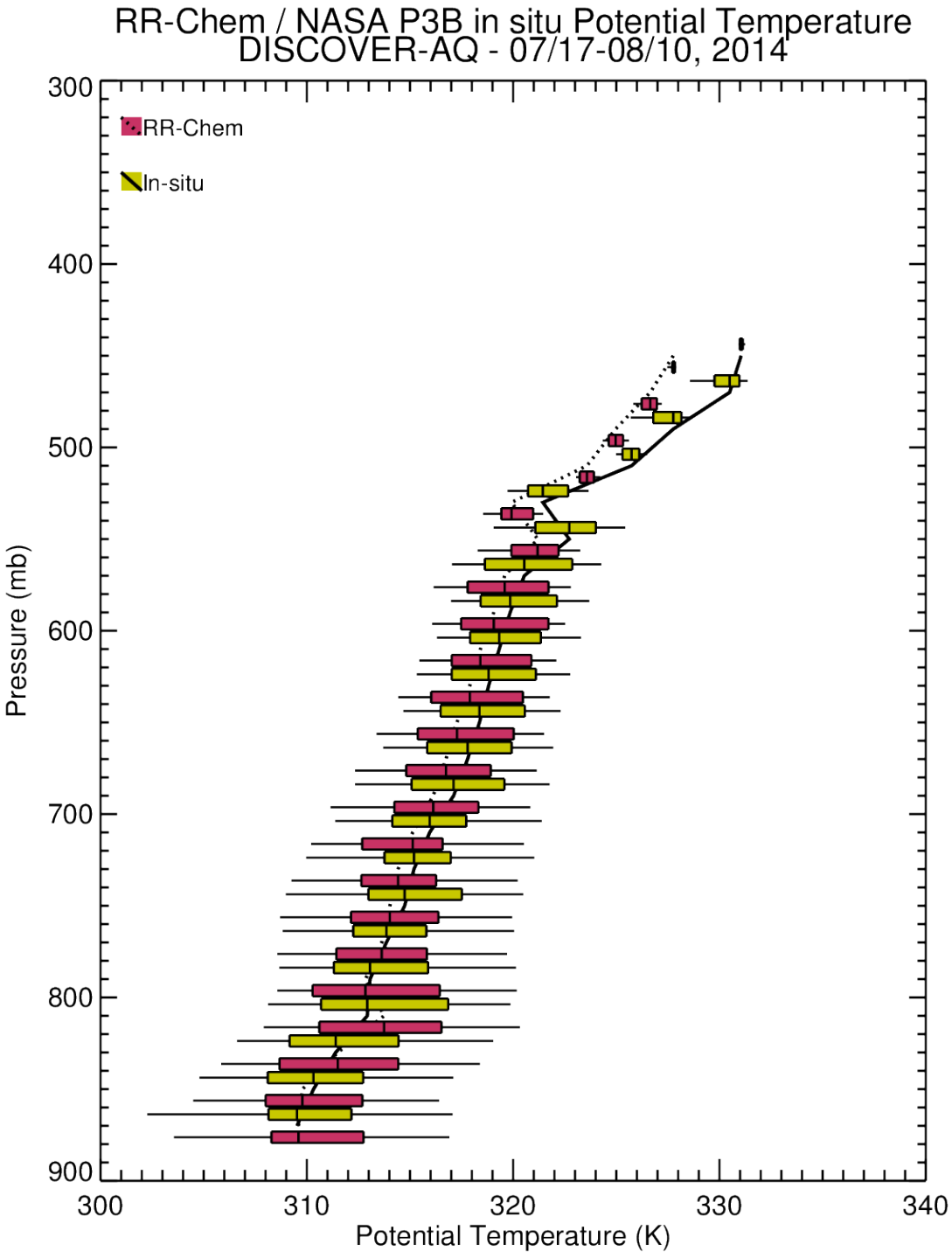

Figure 3.7: P3B in situ vs. RR-Chem potential temperature statistics

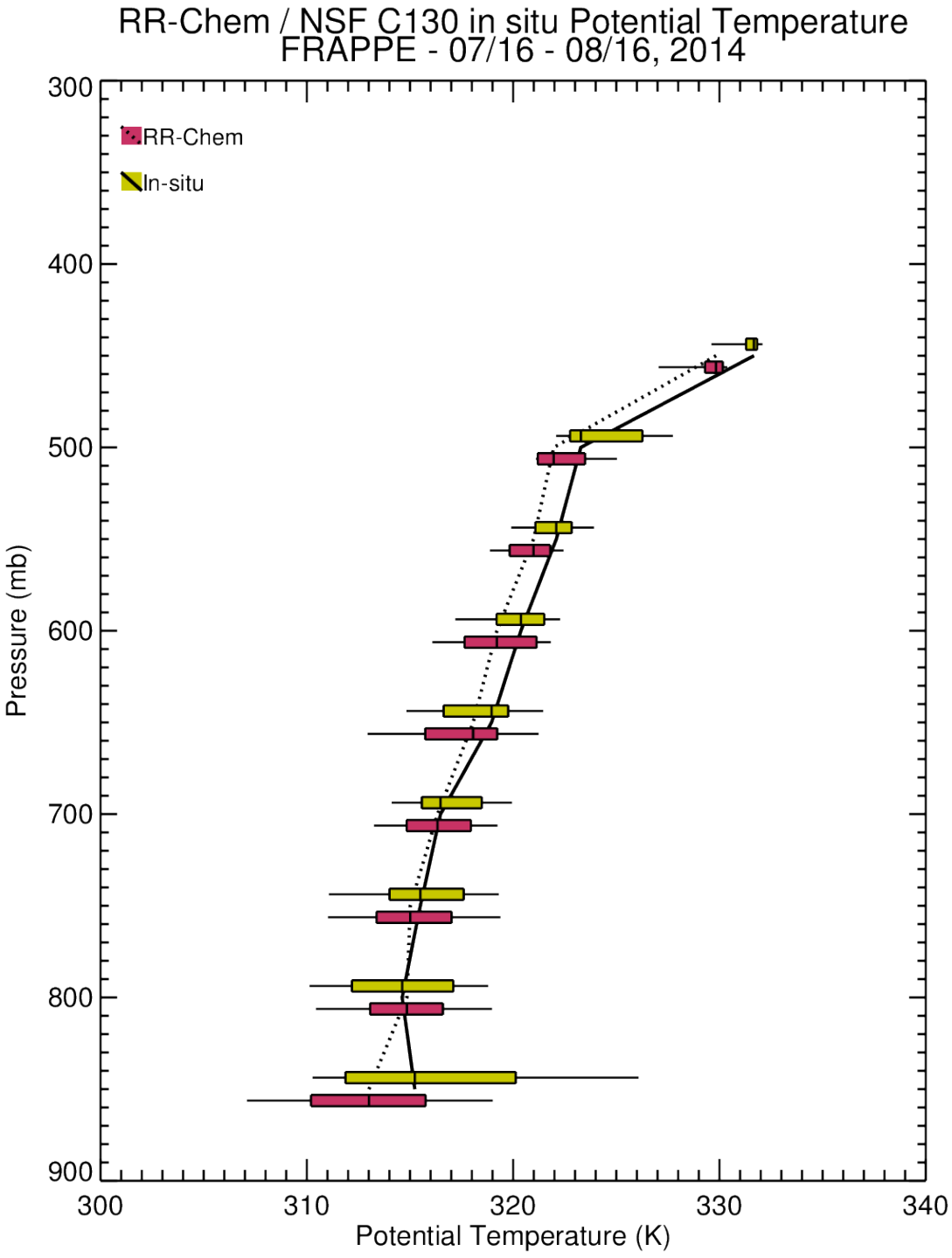

Figure 3.8: C130 in situ vs. RR-Chem potential temperature statistics

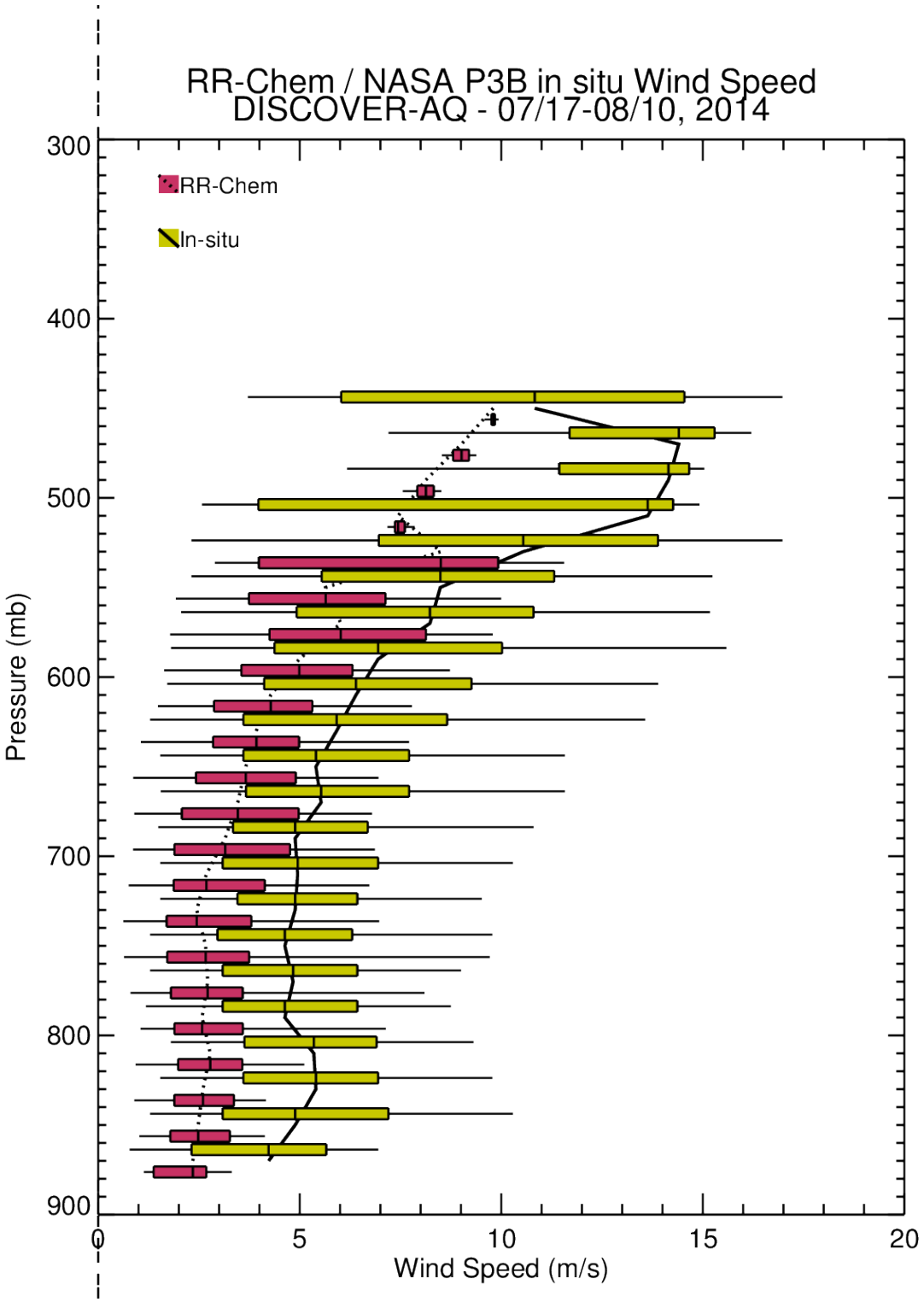

Figure 3.9: P3B in situ vs. RR-Chem wind speed statistics

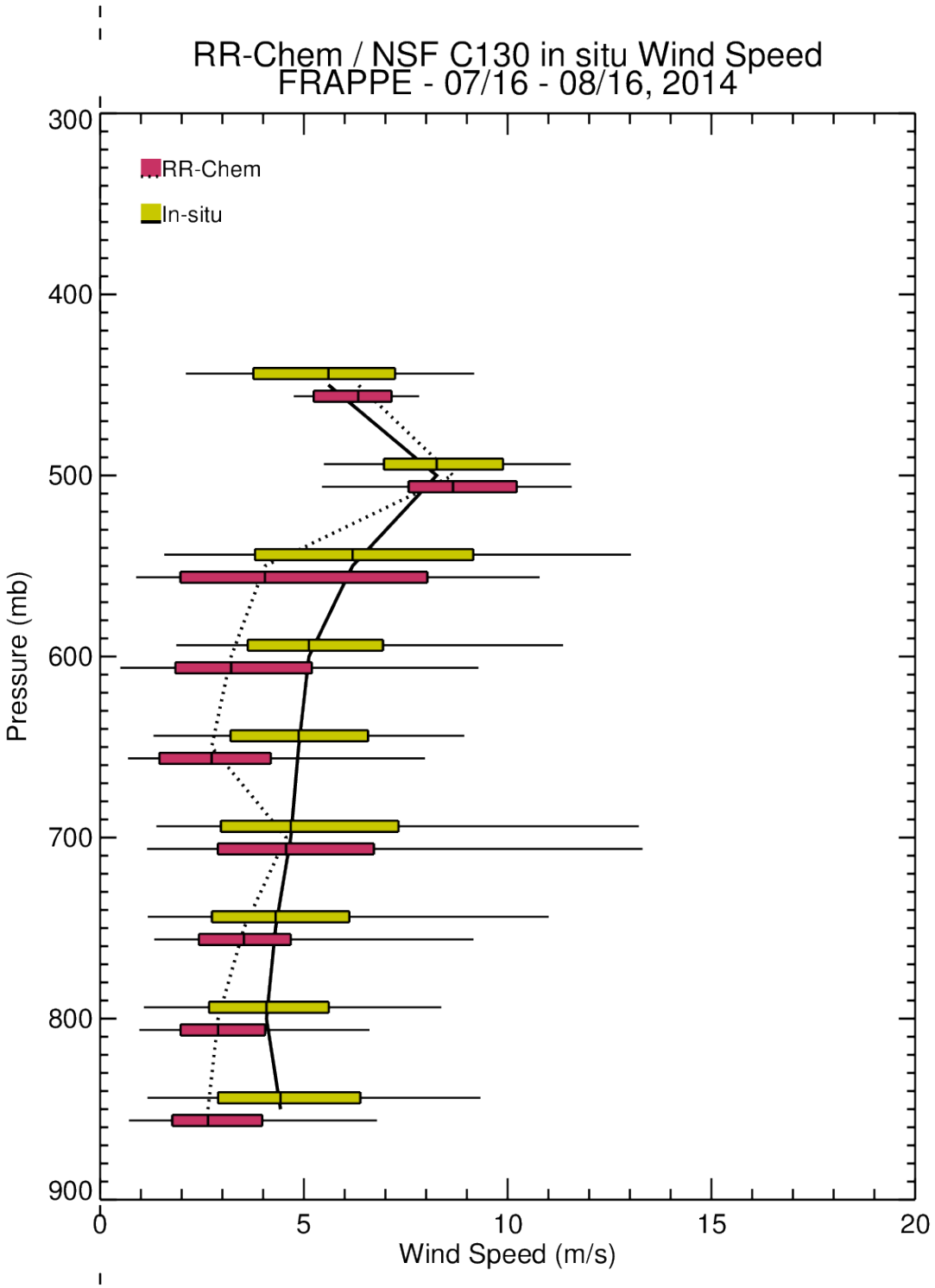

Figure 3.10: C130 in situ vs. RR-Chem wind speed statistics

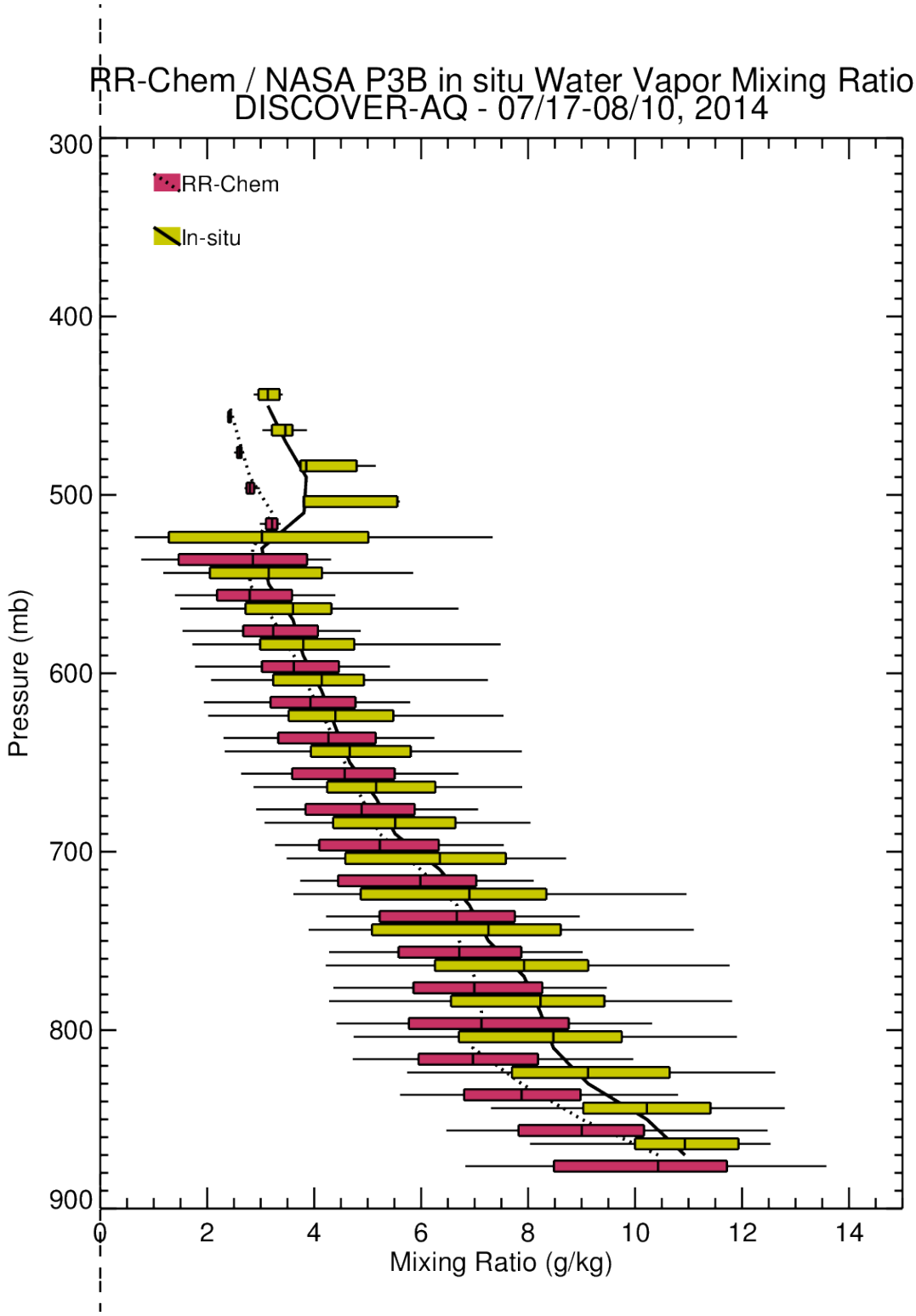

Figure 3.11: P3B in situ vs. RR-Chem potential water vapor mixing ratio statistics

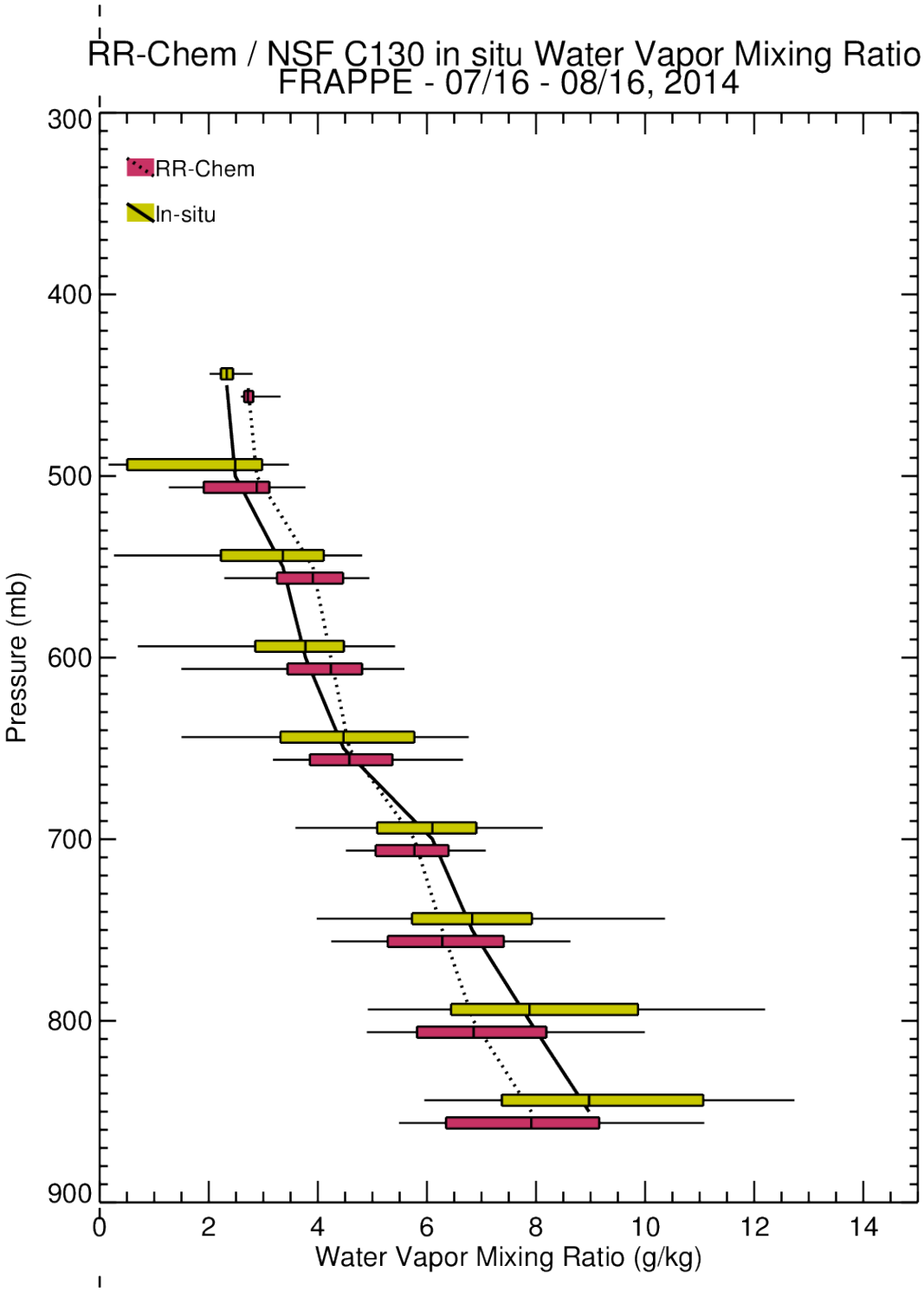

Figure 3.12: C130 in situ vs. RR-Chem potential water vapor mixing ratio statistics

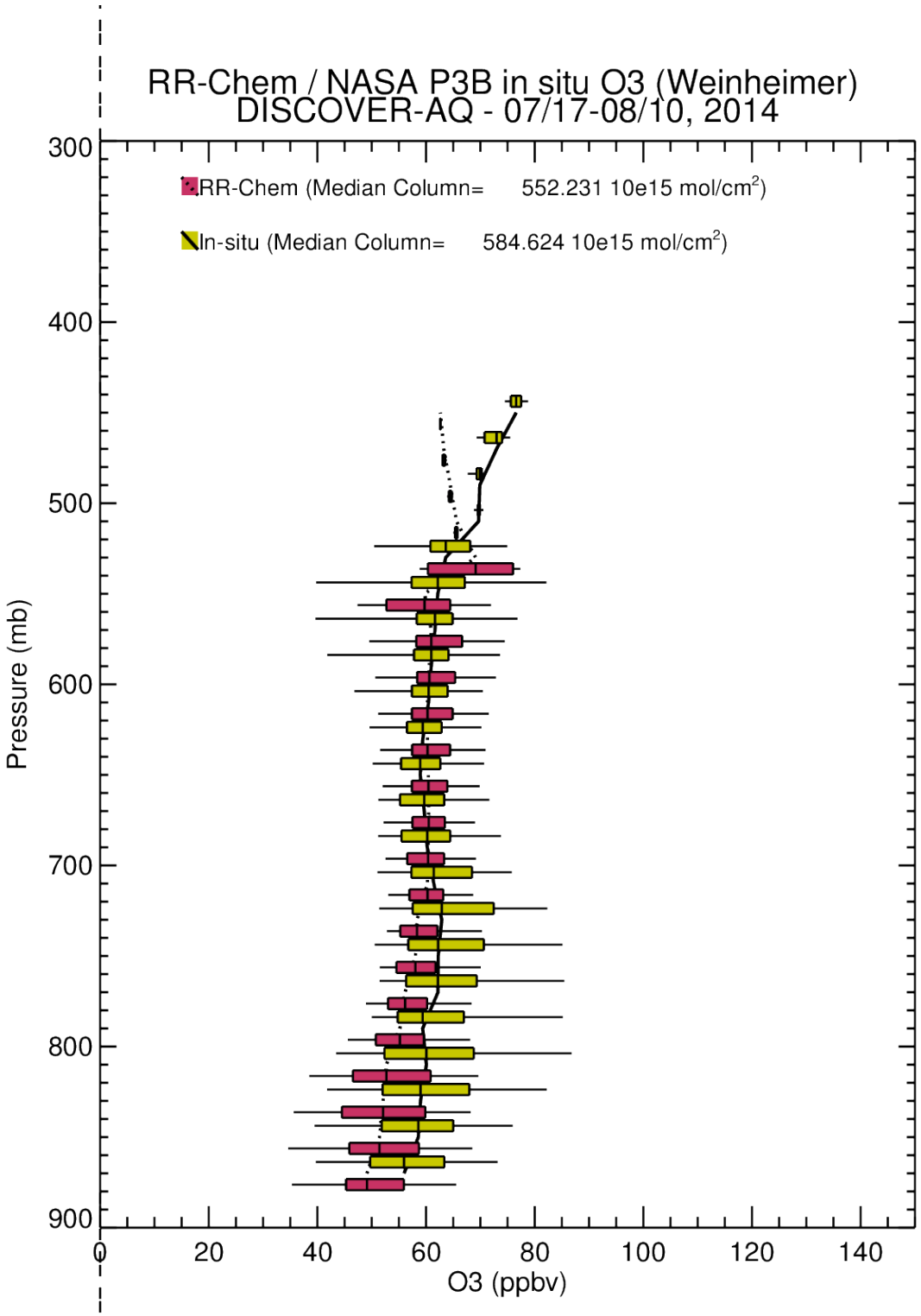

Figure 3.13: P3B in situ vs. RR-Chem O_3 statistics

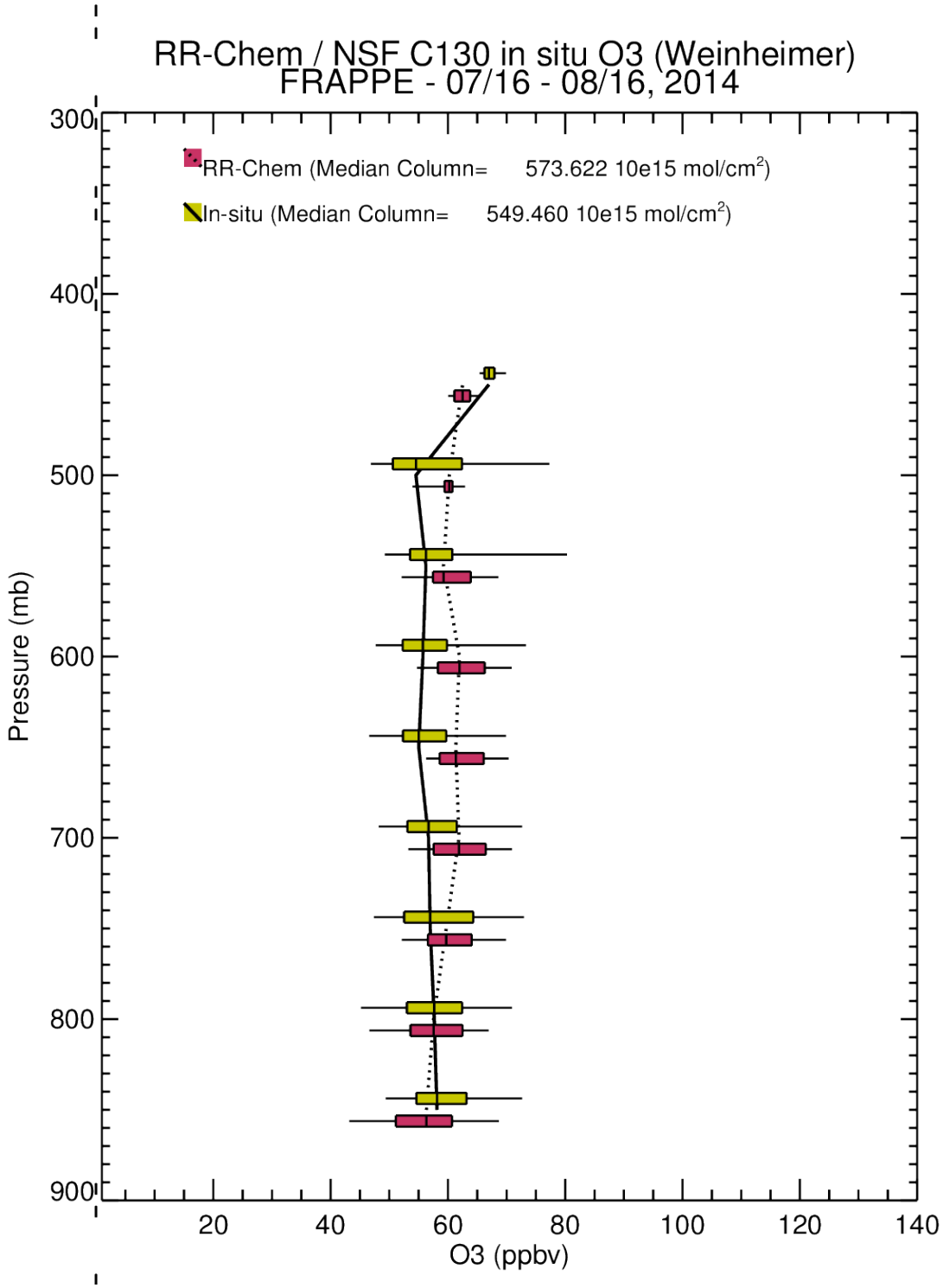

Figure 3.14: C130 in situ vs. RR-Chem O_3 statistics

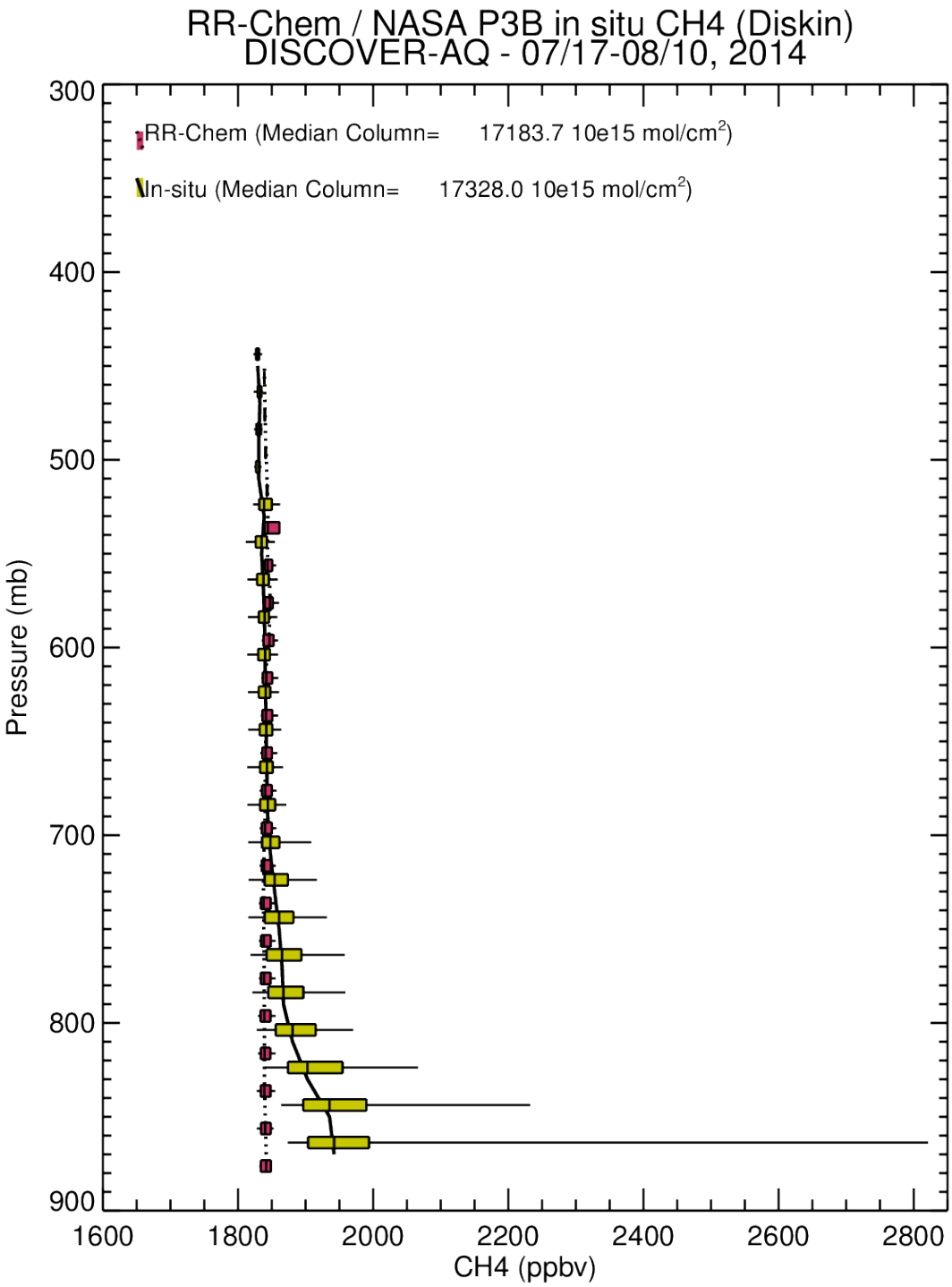

Figure 3.15: P3B in situ vs. RR-Chem CH_4 statistics

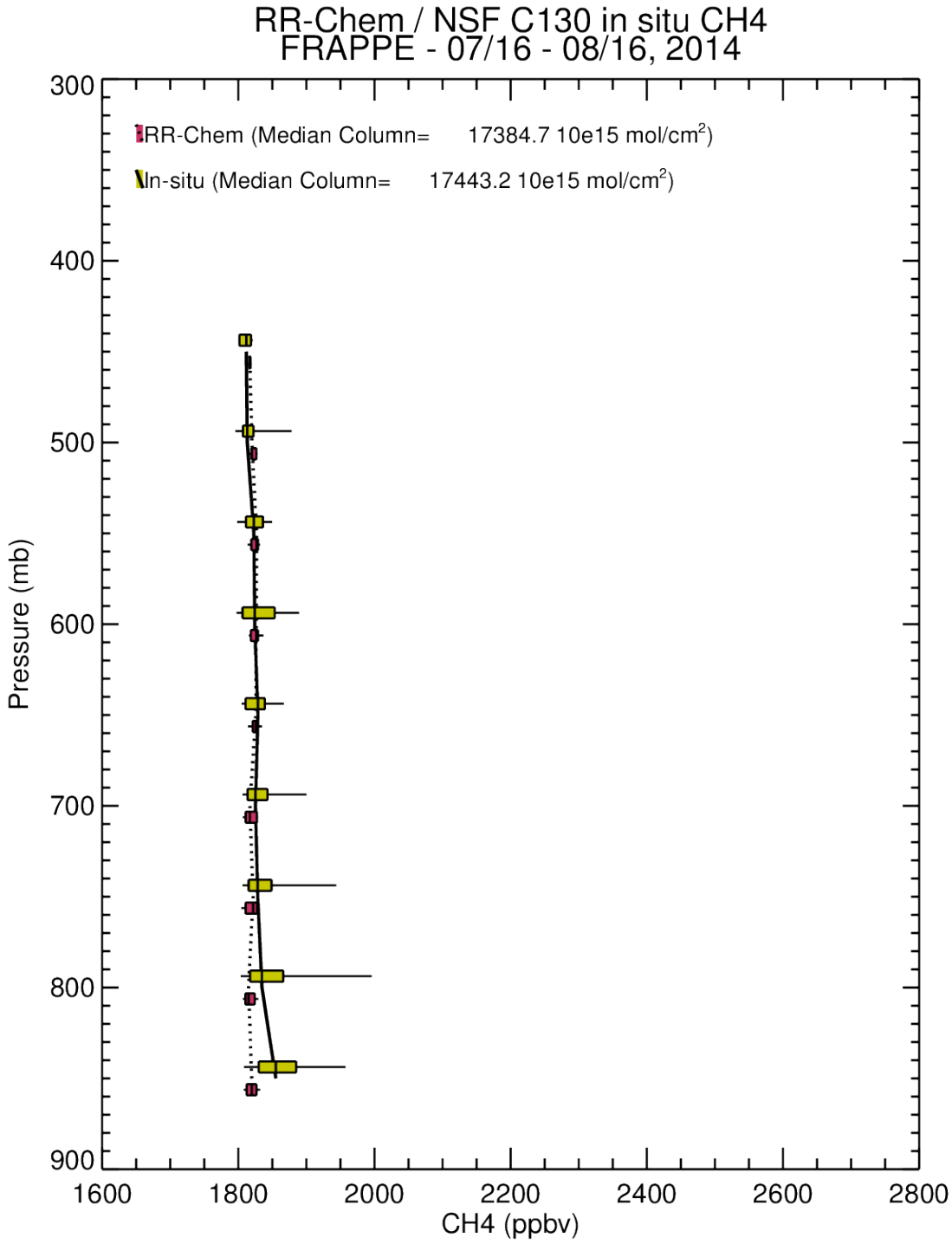

Figure 3.16: C130 in situ vs. RR-Chem CH_4 statistics

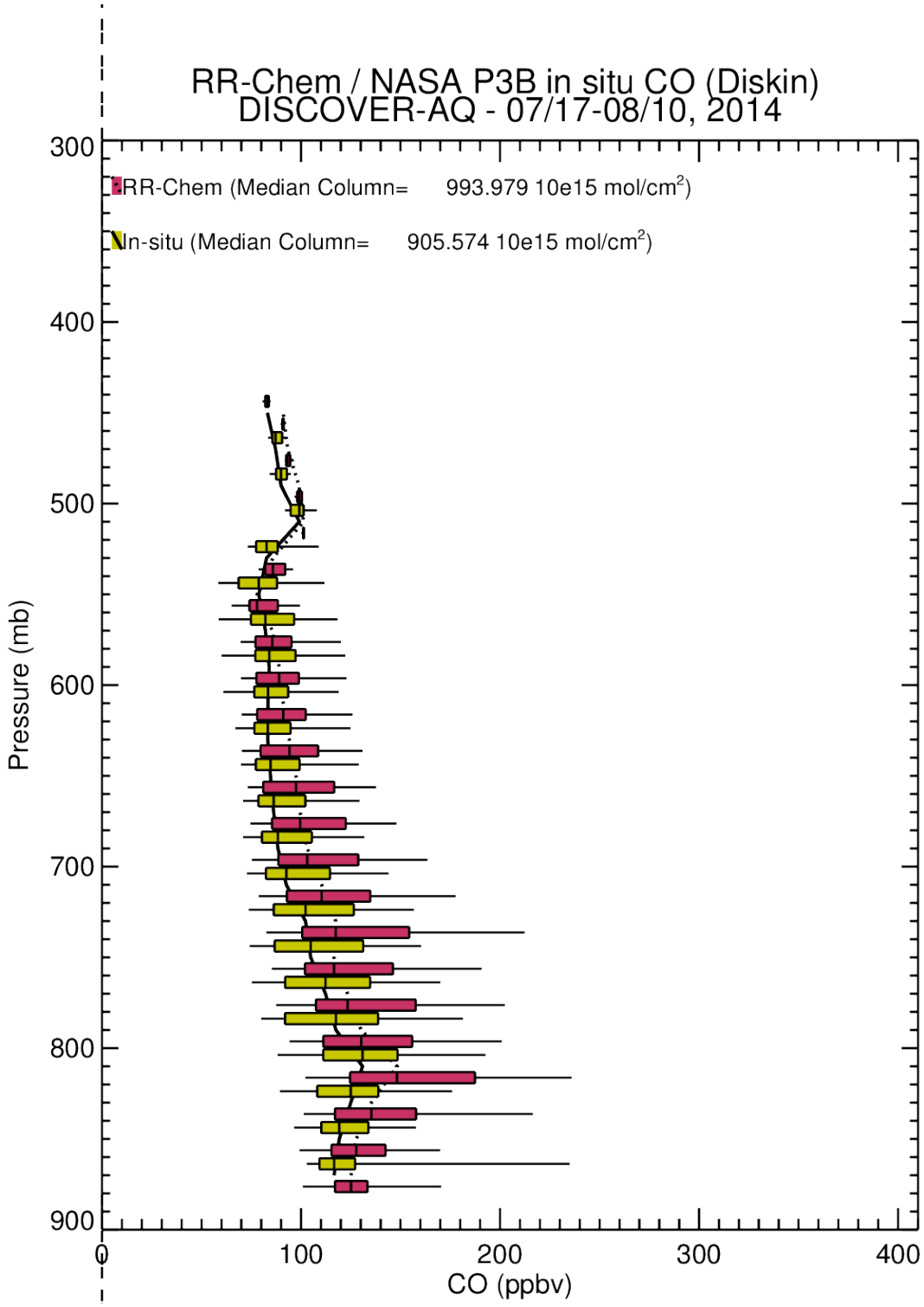

Figure 3.17: P3B in situ vs. RR-Chem CO statistics

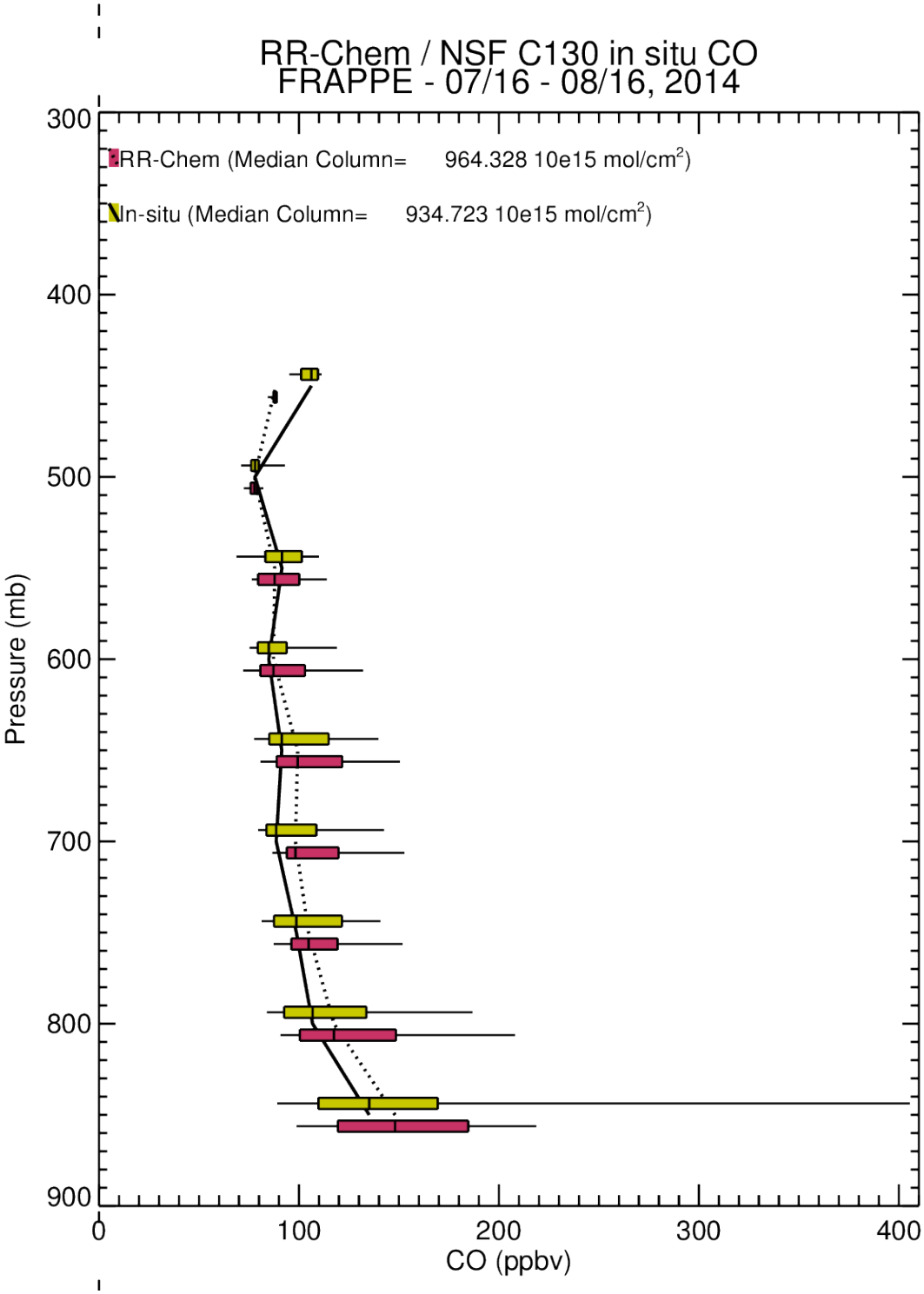

Figure 3.18: C130 in situ vs. RR-Chem CO statistics

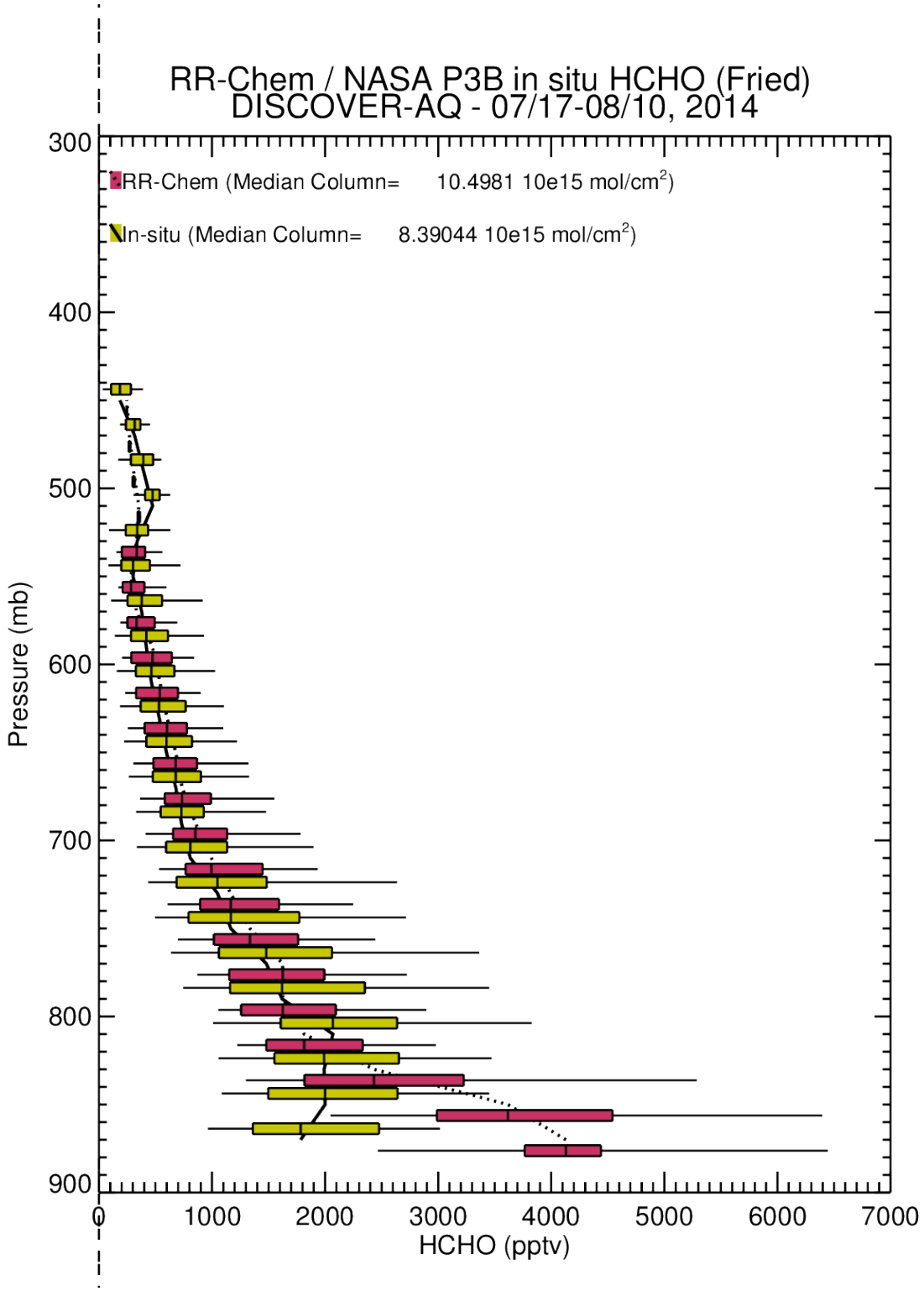

Figure 3.19: P3B in situ vs. RR-Chem HCHO statistics

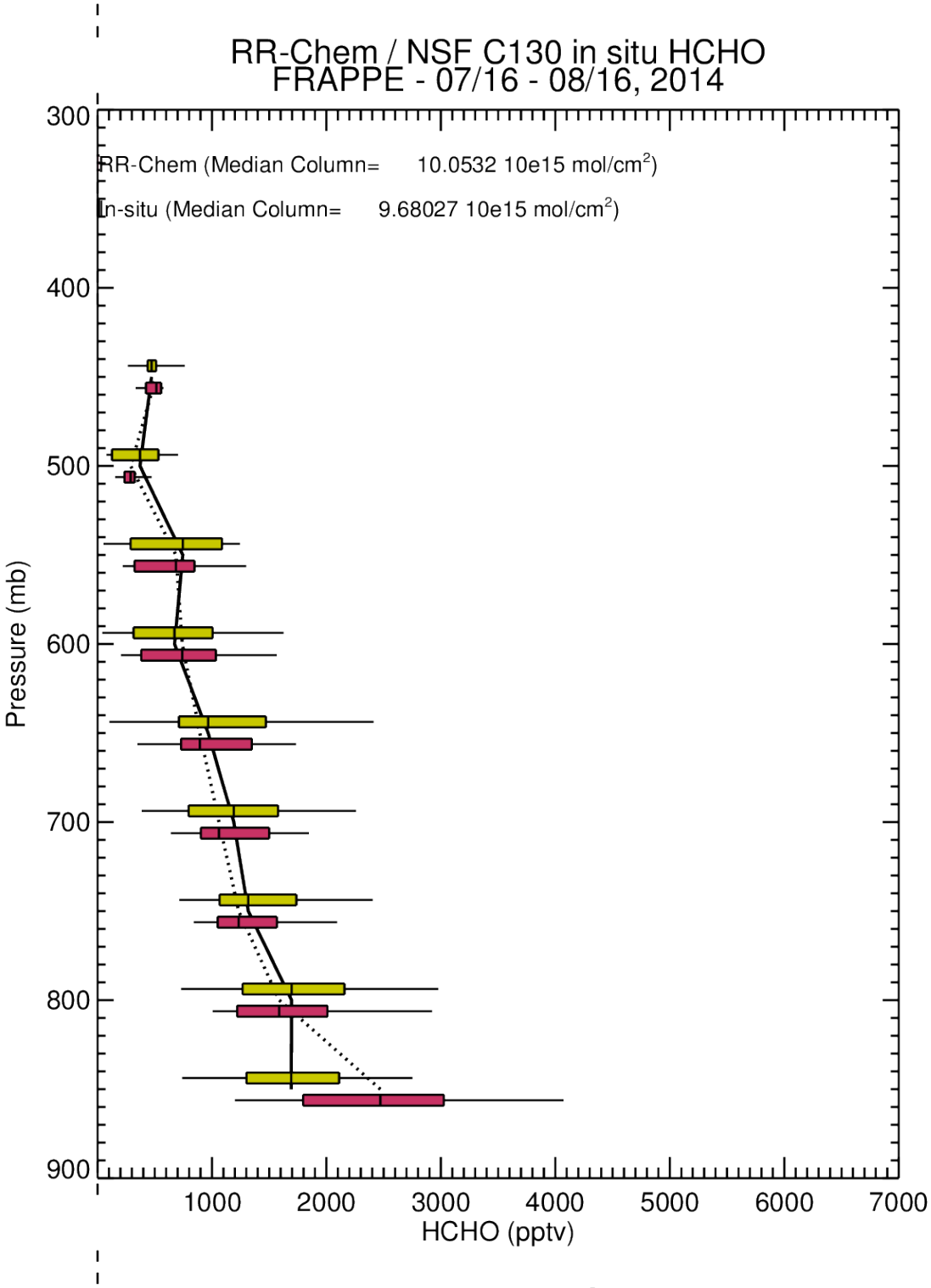

Figure 3.20: C130 in situ vs. RR-Chem HCHO statistics

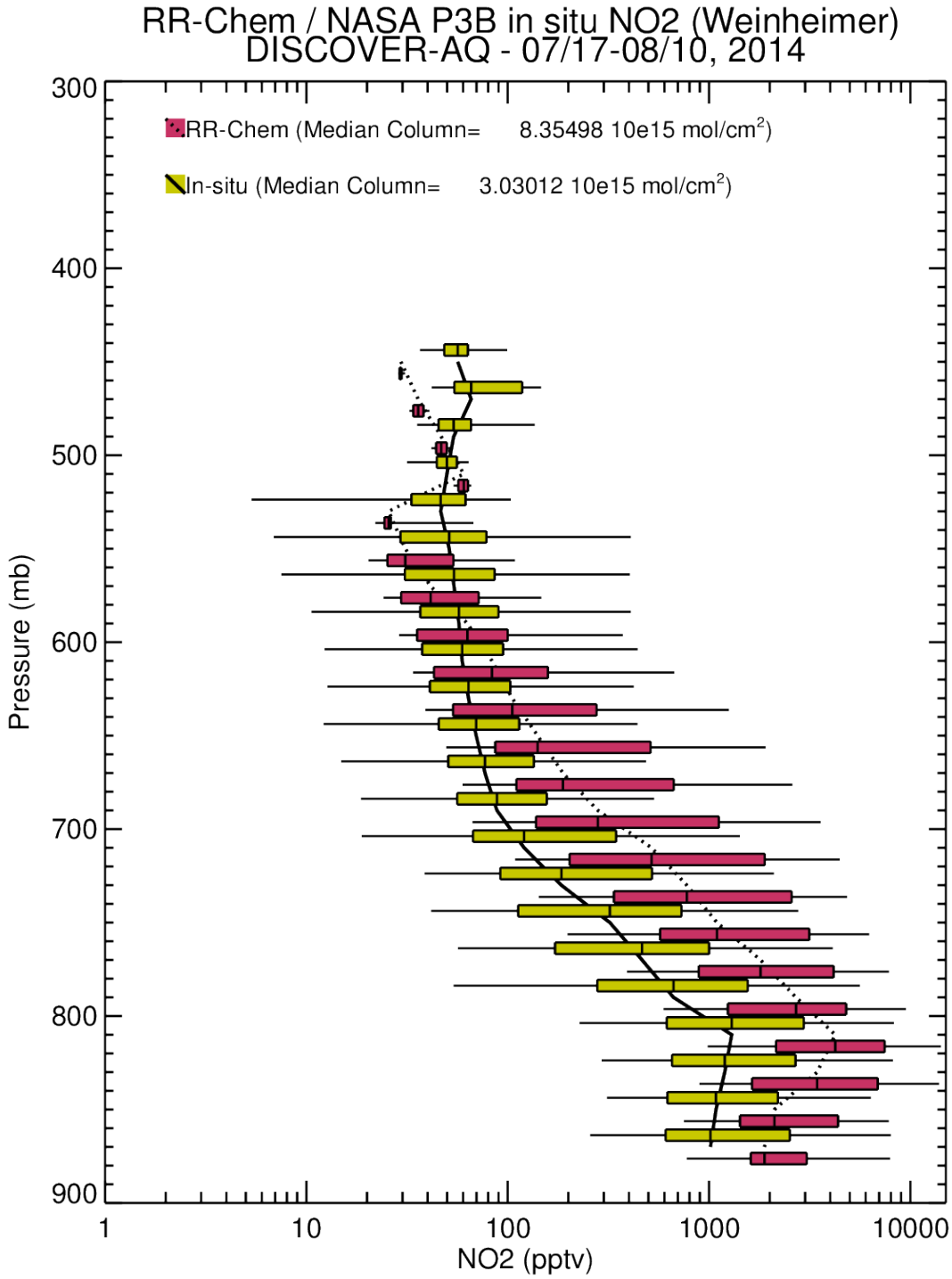

Figure 3.21: P3B in situ vs. RR-Chem NO_2 statistics

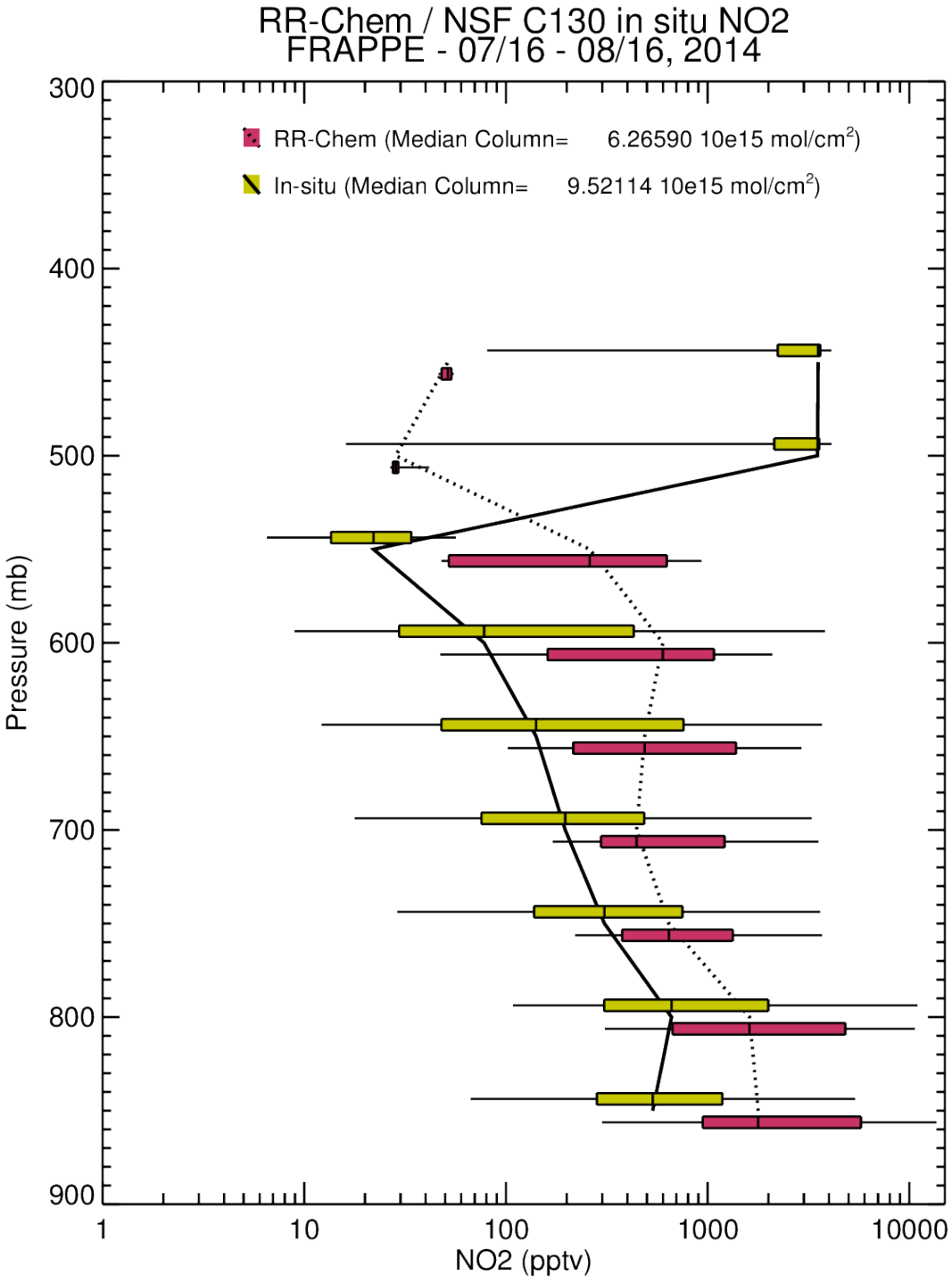

Figure 3.22: C130 in situ vs. RR-Chem NO_2 statistics

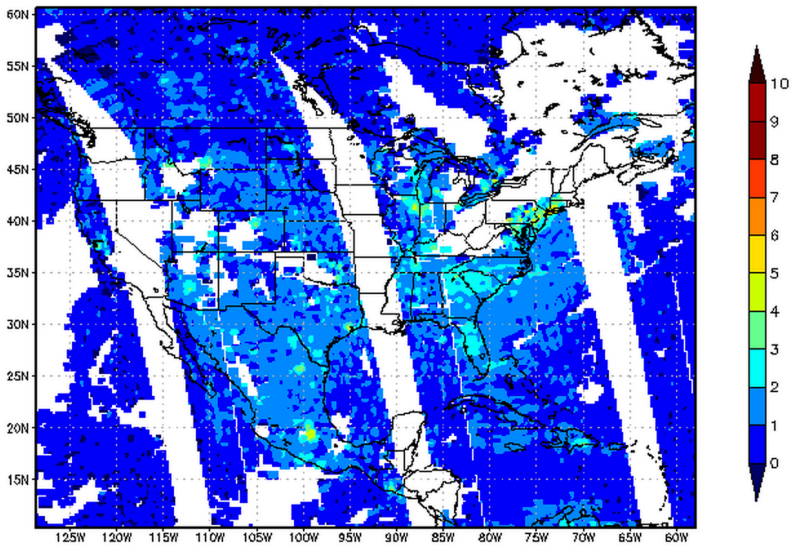

Figure 3.23: OMI tropospheric NO_2 satellite on July 28th, 2014. *Source: NASA, 2014*

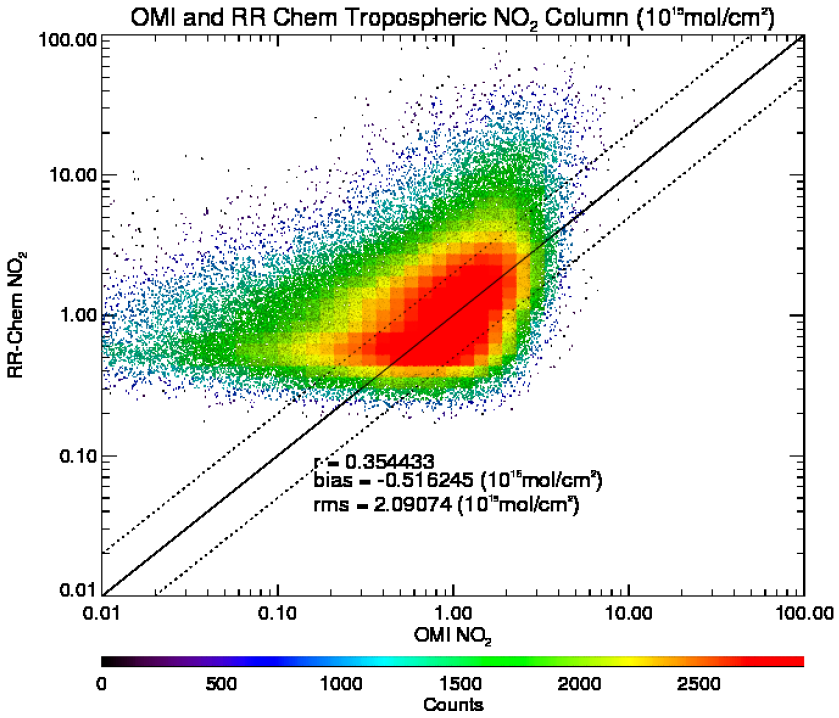

Figure 3.24: OMI vs. RR-Chem tropospheric NO_2 statistics for CONUS

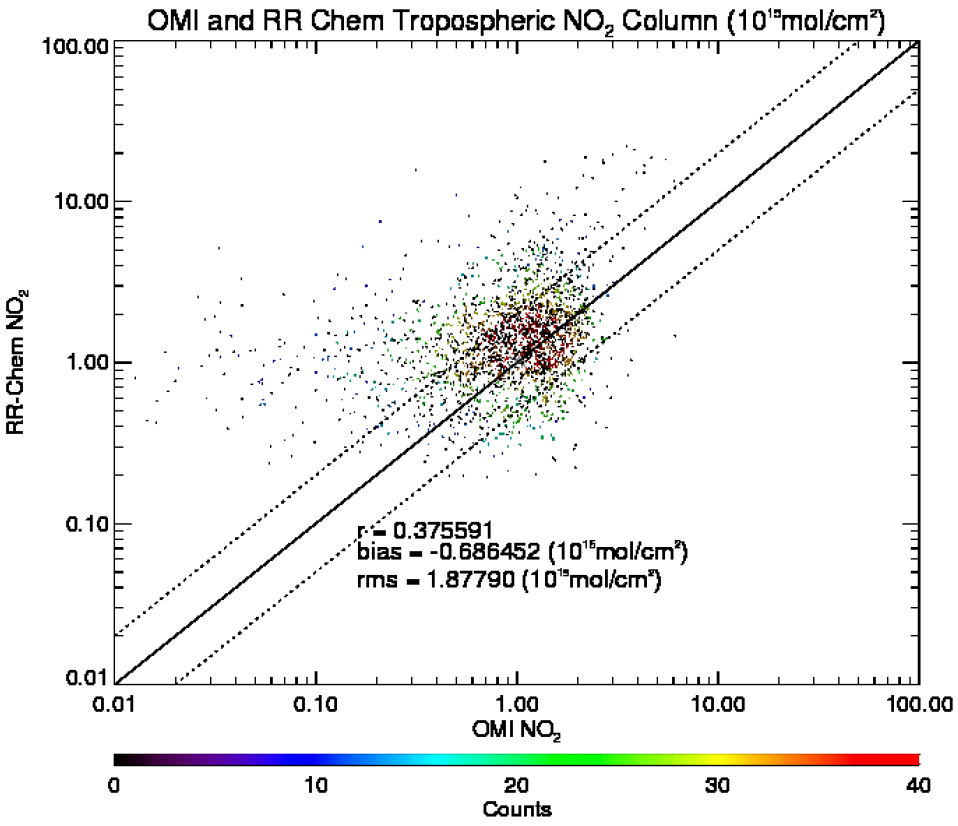

Figure 3.24: OMI vs. RR-Chem tropospheric NO_2 statistics for Colorado

Chapter 3 References

Anderson, D. C., Loughner, C. P., Diskin, G., Weinheimer, A., Canty, T. P., Salawitch, R. J., … Dickerson, R. R. (2014). Measured and modeled CO and NOy in DISCOVER-AQ: An evaluation of emissions and chemistry over the eastern US. Atmospheric Environment, 96, 78–87. doi:10.1016/j.atmosenv.2014.07.004

Barth, M. C., Wong, J., Bela, M. M., Pickering, K. E., Li, Y., & Cummings, K. (2014). Simulations of L ightning - Generated NOx for Parameterized C onvection in the WRF - Chem model, 4(2), 15–20.

Czader, B. H., Li, X., & Rappenglueck, B. (2013). CMAQ modeling and analysis of radicals, radical precursors, and chemical transformations. Journal of Geophysical Research: Atmospheres, 118(19), 11376–11387. doi:10.1002/jgrd.50807

Dye, T. S., AIRNow Program (U.S.), & Sonoma Technology Inc. (2003). Guidelines for Developing an Air Quality (ozone and PM2.5) Forecasting Program, 1.

EPA, U. (2013). 2011 National Emissions Inventory, Version 1 Technical Support Document, (November).

Fast, J. D., Gustafson, W. I., Easter, R. C., Zaveri, R. a., Barnard, J. C., Chapman, E. G., … Peckham, S. E. (2006). Evolution of ozone, particulates, and aerosol direct radiative forcing in the vicinity of Houston using a fully coupled meteorology-chemistry-aerosol model. Journal of Geophysical Research: Atmospheres, 111(21), 1–29. doi:10.1029/2005JD006721

Ghude, S. D., Pfister, G. G., Jena, C., Van Der A, R. J., Emmons, L. K., & Kumar, R. (2013). Satellite constraints of nitrogen oxide (NOx) emissions from India based on OMI observations and WRF-Chem simulations. Geophysical Research Letters, 40(2), 423–428. doi:10.1029/2012GL053926

Grell, G. a., Peckham, S. E., Schmitz, R., McKeen, S. a., Frost, G., Skamarock, W. C., & Eder, B. (2005). Fully coupled "online" chemistry within the WRF model. Atmospheric Environment, 39(37), 6957–6975. doi:10.1016/j.atmosenv.2005.04.027

Jacob, D. (1999). Introduction to atmospheric chemistry. Princeton University Press.

Marshall, J., & Plumb, R. A. (1965). Atmosphere, ocean and climate dynamics: an introductory text (Vol. 8). Academic Press.

McCalla, C. (1981). *Objective Determination of the Tropopause Using WMO Operational Definitions*. US Department of Commerce, National Oceanic and Atmospheric Administration, National Weather Service, National Meteorological Center.

McKeen, S. a., Chung, S. H., Wilczak, J., Grell, G., Djalalova, I., Peckham, S., … Yu, S. (2007). Evaluation of several PM2.5 forecast models using data collected during the ICARTT/NEAQS 2004 field study. Journal of Geophysical Research: Atmospheres, 112(10), 1–20. doi:10.1029/2006JD007608

Saide, P. E., Carmichael, G. R., Spak, S. N., Gallardo, L., Osses, A. E., Mena-Carrasco, M. a., & Pagowski, M. (2011). Forecasting urban PM10 and PM2.5 pollution episodes in very stable nocturnal conditions and complex terrain using WRF-Chem CO tracer model. Atmospheric Environment, 45(16), 2769–2780. doi:10.1016/j.atmosenv.2011.02.001

Simon, H., Baker, K. R., & Phillips, S. (2012). Compilation and interpretation of photochemical model performance statistics published between 2006 and 2012. Atmospheric Environment, 61, 124–139. doi:10.1016/j.atmosenv.2012.07.012

Tie, X., Madronich, S., Li, G., Ying, Z., Zhang, R., Garcia, A. R., … Liu, Y. (2007). Characterizations of chemical oxidants in Mexico City: A regional chemical dynamical model (WRF-Chem) study. Atmospheric Environment, 41(9), 1989–2008. doi:10.1016/j.atmosenv.2006.10.053

Tuccella, P., Curci, G., Visconti, G., Bessagnet, B., Menut, L., & Park, R. J. (2012). Modeling of gas and aerosol with WRF/Chem over Europe: Evaluation and sensitivity study. Journal of Geophysical Research: Atmospheres, 117(3), 1–15. doi:10.1029/2011JD016302

Valin, L. C., Russell, a. R., Hudman, R. C., & Cohen, R. C. (2011). Effects of model resolution on the interpretation of satellite NO2 observations. Atmospheric Chemistry and Physics, 11(22), 11647–11655. doi:10.5194/acp-11-11647-2011

Yerramilli, A., Challa, V. S., Dodla, V. B. R., Dasari, H. P., Young, J. H., Patrick, C., … Swanier, S. J. (2010). Simulation of Surface Ozone Pollution in the Central Gulf Coast Region Using WRF/Chem Model: Sensitivity to PBL and Land Surface Physics. Advances in Meteorology, 2010, 1–24. doi:10.1155/2010/319138

Ying, Z., Tie, X., & Li, G. (2009). Sensitivity of ozone concentrations to diurnal variations of surface emissions in Mexico City: A WRF/Chem modeling study. Atmospheric Environment, 43(4), 851–859. doi:10.1016/j.atmosenv.2008.10.044

Žabkar, R., Honzak, L., Skok, G., Forkel, R., Rakovec, J., Ceglar, a., & Žagar, N. (2015). Evaluation of the high resolution WRF-Chem air quality forecast and its comparison with statistical ozone predictions. Geoscientific Model Development Discussions, 8(2), 1029–1075. doi:10.5194/gmdd-8-1029-2015

Zhang, Y., Chen, Y., Sarwar, G., & Schere, K. (2012). Impact of gas-phase mechanisms on Weather Research Forecasting Model with Chemistry (WRF/Chem) predictions: Mechanism implementation and comparative evaluation. Journal of Geophysical Research: Atmospheres, 117(1), 1–31. doi:10.1029/2011JD015775

Chapter 4: A Case Study of Elevated Observed Ground-level Ozone

The field campaign, while successful in its goals, observed fewer than expected days of pollutant concentrations reaching above the NAAQS limit for ozone of an average of 75 ppb over 8 hours. Cooler than expected temperatures and rain in Colorado and the Front Range during the campaigns likely caused the abnormally low number of days with high ozone.

Despite the unexpected weather, several high ozone concentration periods were observed in the Front Range area. In particular, we have focused on the highest observed ozone concentrations at the Boulder Atmospheric Observatory Tower, an episode that stretched over two days from July 28 to July 29, 2014. During this high ozone episode, concentrations peaked just above 75ppb on the 28th and above 80ppb on the 29th. This specific episode is also of interest since models forecasted the dynamic gyre known as the Denver Cyclone centered near BAO Tower during the morning and early afternoon of July 28th.

On July 28th, the official FRAPPE Field Report for the day read, “On this day, ozone levels rose more broadly across the ground stations at the profile locations, with the exception of Fort Collins which was outside the cyclone

circulation. While ozone increased steadily across the region, the usual afternoon storms began moving into the area and tornado activity was reported east of Denver and in Platteville." With this report, we know that a Denver Cyclone was observed and there was a significant gradient of ozone between the interior and exterior of the gyre. Given the field report, we utilize a variety of measurements and reports including model data, surface observations, and *in situ* observations made by both the P3B and the C130 to perform a thorough analysis of the model performance on this particular episode.

Surface Observation Analysis

Starting at 9am on July 28th, AirNow stations across the Front Range started to deviate from the modeled surface ozone with modeled concentrations remaining in the 40 ppb to 50 ppb range while observation stations rose into the 60ppb range (Figure 4.1; Figure 4.3). By the time the next model output was generated 3 hours later at 12pm, modeled ozone had risen most prominently east of the Rocky Mountains with concentrations ranging from 40 ppb to 70 ppb (Figure 4.4). Despite the elevation of ozone concentration expected with the typical diurnal pattern of ozone formation and destruction, AirNow stations reported concentration well above 80ppb around the Denver Metropolitan area

with lower concentrations near 70ppb near Fort Collins, but still higher than what was modeled for the region. For the next model forecast at 3pm, predicted ozone concentrations had formed a local high in the Fort Collins region consistent with AirNow stations that also observed higher concentrations in the area (Figure 4.5). Unlike modeled results, AirNow stations for the region remained 10ppb to 20ppb higher than what was predicted. Closer to the Denver area and Colorado Springs areas, observed ozone concentrations had fallen closer in line with the RR-Chem model with readings from 40ppb to 50ppb (Figure 4.6).

Based on the comparisons between the model and observations across Colorado, several conclusions can be made. One, when this exceptionally high ozone event occurred, the RR-Chem model was able to capture the general temporal scale when the event occurred but was unable to capture the intensity of the event. Based on the field catalog observations, the Denver Cyclone may have contributed to enhancement of near surface ozone concentrations due to entrainment within the gyre. Similarly, for stations south of Denver, the observed values were much closer to what was predicted indicating there may be a problem modeling urban chemistry or the dynamics of the Denver Cyclone and associated changes in air chemistry.

At BAO Tower, the temporal peaks of the forecasted maximum ozone concentrations for both days were delayed by two to three hours relative to observations. Like AirNow, BAO Tower saw maximum concentrations some 20ppb greater than what RR-Chem forecasted. During the evening and early morning, the modeled temporal minimum in ozone concentration was later than what was observed, however, there was much less of a bias than during the day for this particular case study. The modeled cross section of BAO Tower shows high ozone aloft, likely of stratospheric origin, above 8km above ground level (AGL) with lesser enhancement near the surface (Figure 4.2).

Aircraft Comparison

The P3B aircraft made two flights on the 28th and one flight on the 29th over the Front Range (Figure 4.8). The first of the flights on the 28th lasted from approximately 8am to 1pm with 5 significant changes in elevation. The 9am, 10am, and 11am flights all saw ozone steadily rise as the aircraft also rose in height from 2km to just under 6km.

Formaldehyde

Over the course of the three flights spanning July 28th and 29th, formaldehyde measurements were only recorded on the first flight on the 28th. Most notably, overprediction of HCHO is evident close to the surface (Figure 4.9). As the aircraft ascended, modeled concentrations were better correlated and had very little bias. The lack of correlation and high bias of the model closer to the surface would point to the incorrect modeling of anthropogenic sources. Similar to the general *in situ* findings, previous studies have found underestimation of HCHO by models (Barth et al., 2014; Czader et al., 2013) while this study shows an overestimation that could reflect a problem with the NEI 2011 HCHO emissions in the model.

Nitrogen Dioxide

Over the course of both flights on the 28th, nitrogen dioxide predictions were only slightly better correlated to airborne observations than formaldehyde. Also like formaldehyde, nitrogen dioxide was greatly overestimated by the model with the exception of several spikes in measurements. The RR-Chem model tended to predict the highest values of NO_2 in the morning with less accurate forecasts of concentrations later in the day (Figure 4.10; Figure 4.11).

Unlike the model, observations showed no observable diurnal trend. Again like formaldehyde, nitrogen dioxide biases were largest closer to the surface suggesting the modeled bias is likely due to emissions. Like formaldehyde, previous works have also noted a high bias of WRF-Chem modeled NO_2 most likely associated with the NEI 2011 database (Anderson et al., 2014; EPA, 2013; Ghude et al., 2013; Valin et al., 2011).

Ozone

During the morning aircraft spirals, ozone typically rose from approximately 50ppb to 75ppb, whereas the later spirals at 12pm show little enhancement as the aircraft rose with *in situ* observations recording 60ppb to 80ppb from 12pm until the flight landed at 1pm (Figure 4.12). Typically, the modeled O3 following the aircraft's track saw similar rises in ozone concentration compared to *in situ* during the morning spirals but the model underpredicted ozone by approximately 5ppb to 10ppb during the afternoon spirals, consistent with the surface comparisons. Near the end of the first P3B flight, the model began to deviate to a greater degree from *in situ* observations with a low bias of 20ppb. The smaller vertical concentration gradient observed in the later morning and early afternoon would point to a strong boundary layer

leading to greater mixing and more homogenous ozone concentrations. The failure of the model to capture this raises questions regarding the parameterization of boundary layer mixing within RR-Chem.

The second P3B flight on July 28 took off at 2pm and landed at 5pm with three spirals along the flight track. Like the later spirals by the first P3B flight on the 28th, less enhancement of ozone concentrations were observed as the plane ascended (Figure 4.13). Similarly, the model also predicted little change in ozone concentration during the spirals indicating the boundary layer was likely being modeled correctly. Despite this, the model underpredicted ozone concentrations by approximately 20ppb throughout the entire flight.

Boundary Layer Analysis

Employing the Environmental Protection Agency's (EPA) ceilometer (Charles et al., 1970) to measure boundary layer height, RR-Chem's parameterized boundary layer was further investigated. On both July 28th and July 29th, the modeled boundary layer reached its temporal maximum during the same hour as the ceilometer observed a maximum (Figure 4.15). On the 28th, the modeled boundary layer was slightly lower, 150m, compared to EPA observations. On July 29th the RR-Chem model overpredicted the boundary

layer height by approximately 400m. During the evenings and early morning before both case study days, the EPA's ceilometer observed an uncharacteristically high boundary layer ranging from 1000m to nearly 3500m.

Using the University of Wisconsin's High Spectral Resolution Lidar (UW-HSRL) aerosol backscatter was measured at the BAO Tower site during both early mornings to further investigate the cause of the ceilometer's abnormally high boundary layer measurements (Gross et al., n.d.). In the very early hours of July 28th at BAO Tower UW-HSRL detected a thin cloud layer at approximately 3500m, the same height where the ceilometer detected a boundary layer. Indeed the ceilometer misattributed a low cloud layer as the boundary layer for both nights. When a complete time series of RR-Chem boundary layer output and EPA ceilometer data were compared and analyzed for the entirety of the field campaigns, the correlation was 0.32, the model had a low bias of 277 meters, and the root mean squared error was 1293 meters (Figure 4.14). Based on the inaccurate nighttime measurements made by ceilometer, statistics were recalculated without evening and early morning data. For the same data set, excluding nighttime measurements, correlation improved to 0.70, the bias of the model became high at 415 meters, and the root mean squared error was reduced to 959 meters.

Case Study Discussion

Despite the overall good agreement between modeled and observed ozone throughout the field campaigns, for the highest observed period of ozone, the RR-Chem model failed to capture the observed magnitude and vertical variation. The lack of modeled concentration gradient points to a boundary layer parameterization problem. Upon further investigation, the boundary layer, while temporally delayed, was fairly well predicted during the course of the two day high ozone episode (Figure 4.16). Consequently, it appears that errors in modeling of ozone precursors and the relatively coarse horizontal resolution that may not have been able to properly simulate local dynamics are much more likely causes of the discrepancy between the model and observations during this high ozone event.

Chapter 4 Figures

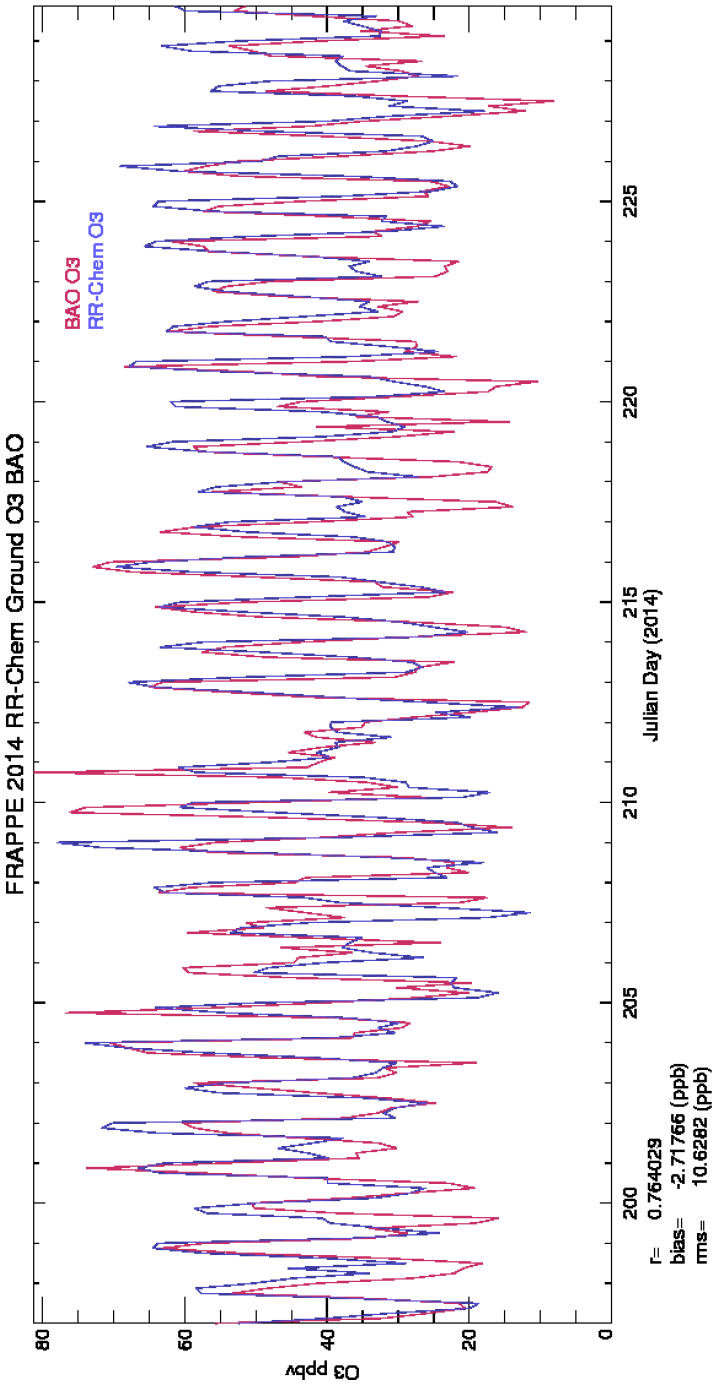

Figure 4.1: BAO Tower vs. RR-Chem O_3 time series and statistics

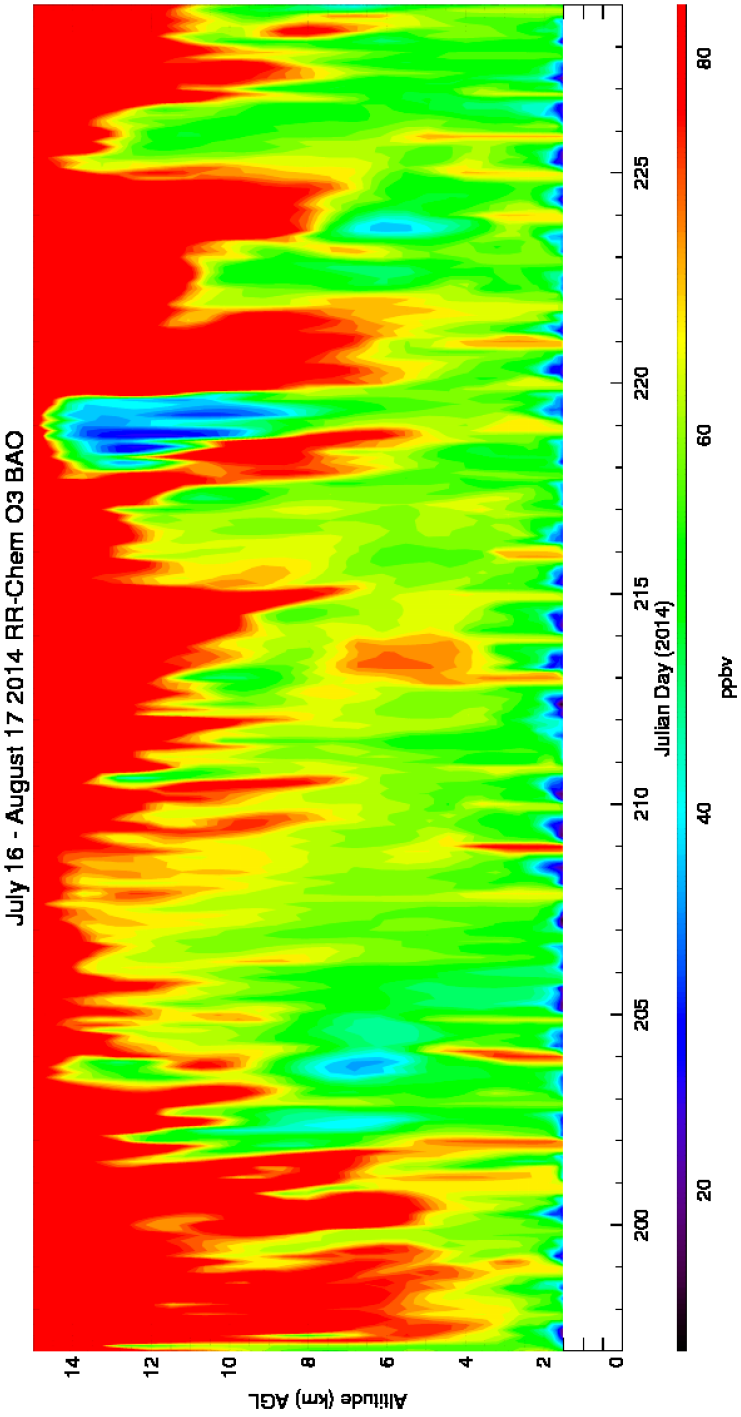

Figure 4.2: RR-Chem O_3 vertical cross-section time series

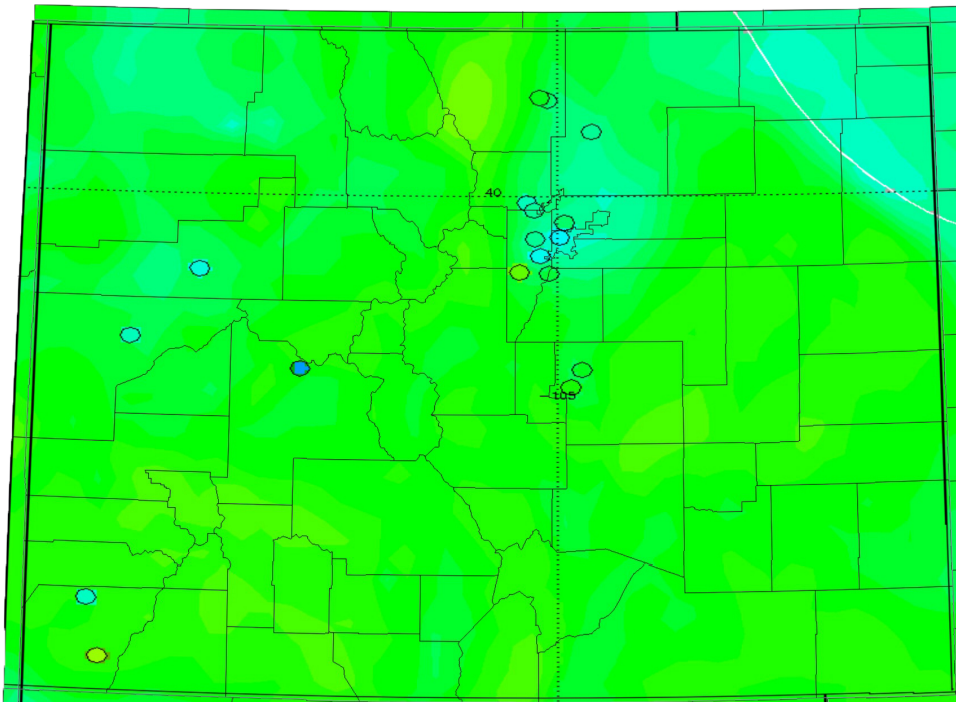

Figure 4.3: AirNow vs. RR-Chem O_3

9 AM, July, 28th, 2014

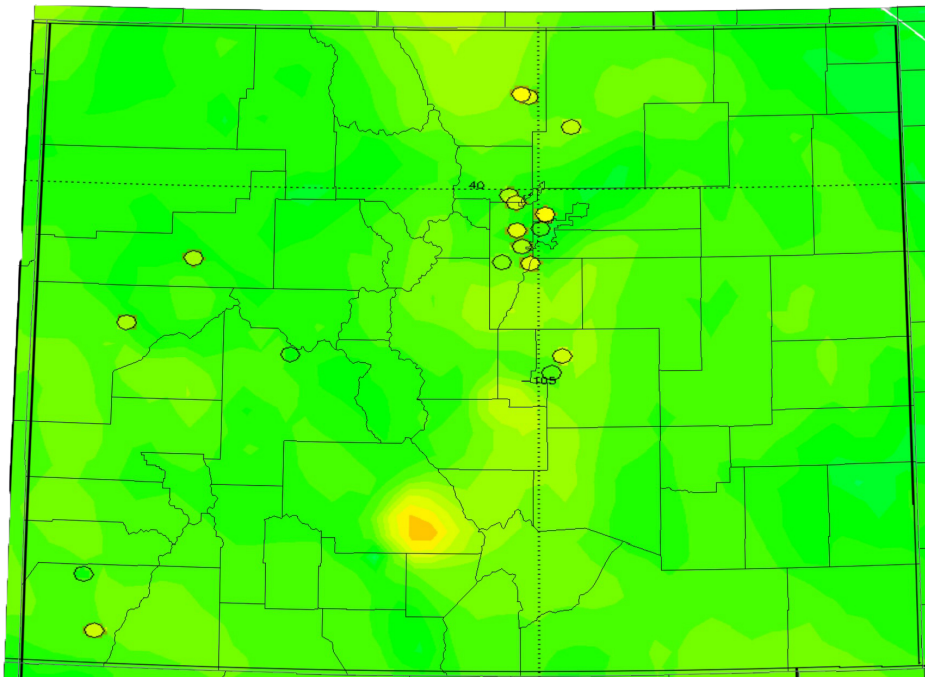

Figure 4.4: AirNow vs. RR-Chem O_3

12 PM, July 28th, 2014

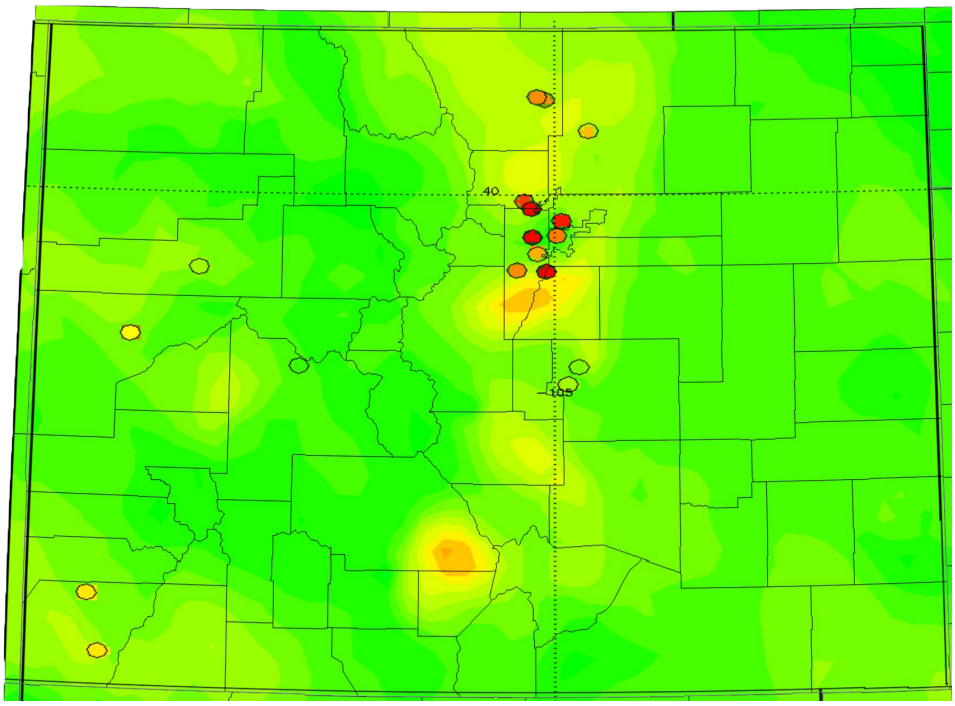

Figure 4.5: AirNow vs. RR-Chem O_3

3 PM, July 28th, 2014

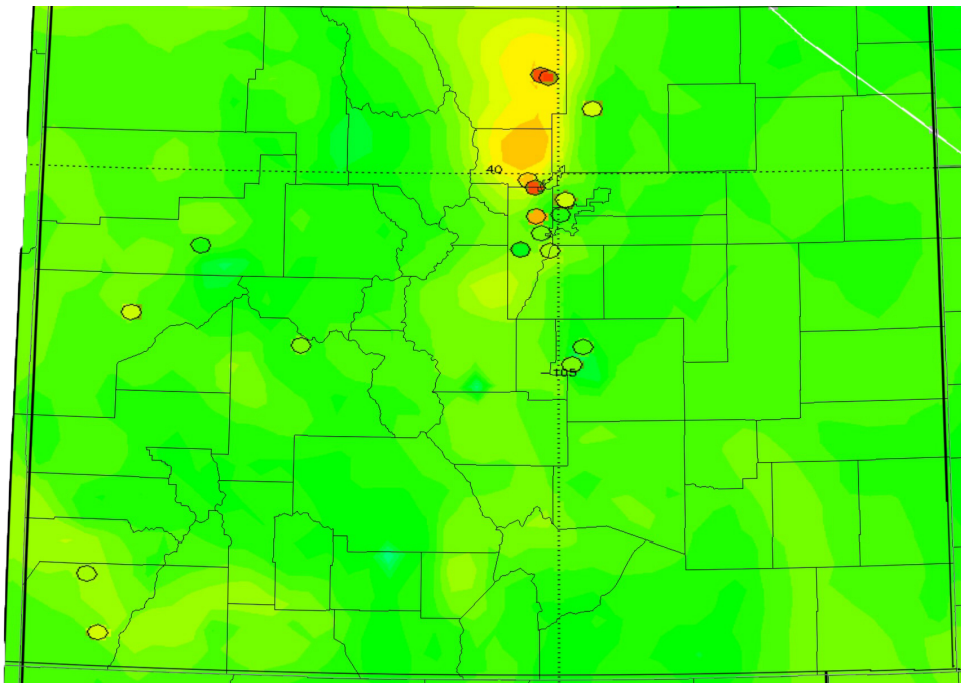

Figure 4.6: AirNow vs. RR-Chem O_3

6 PM, July 28th, 2014

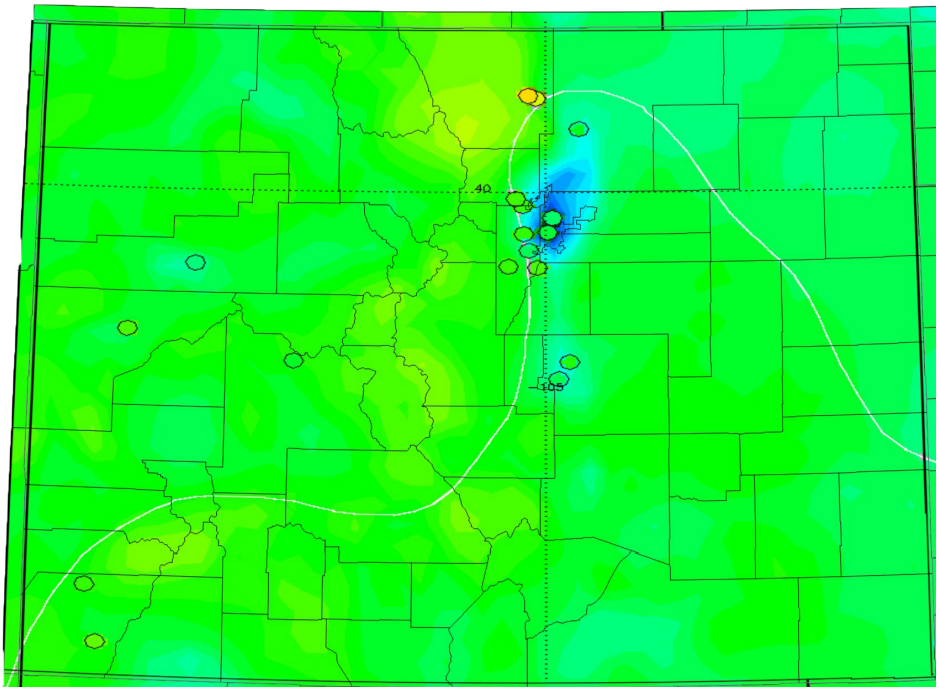

Figure 4.7: AirNow vs. RR-Chem O_3

9 PM, July 28th, 2014

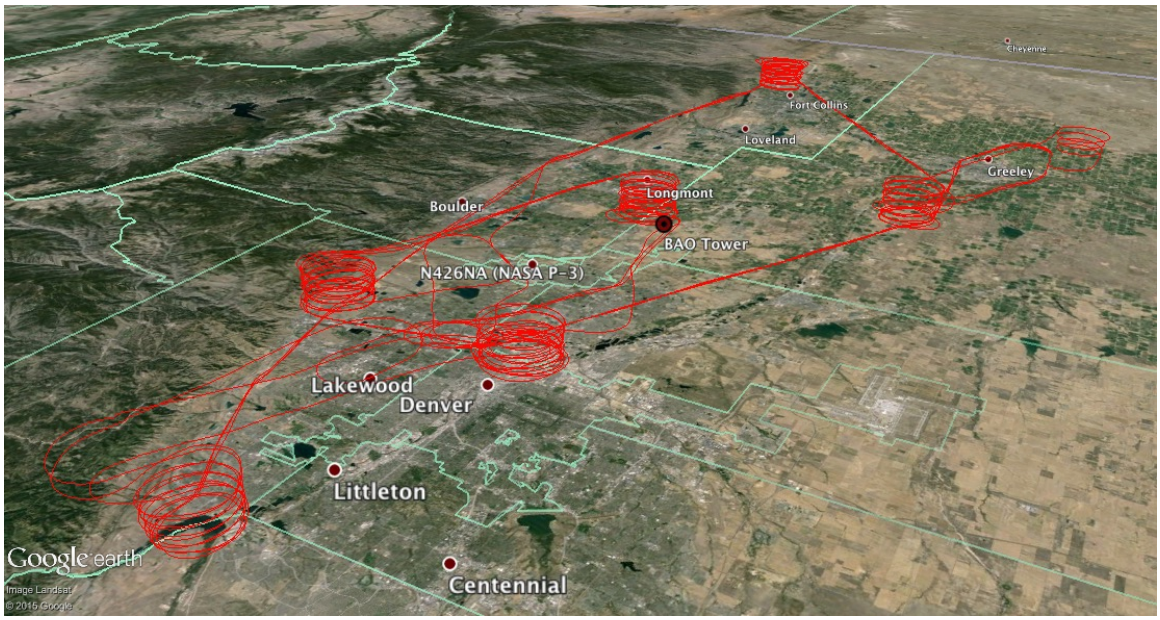

Figure 4.8: P3B flight track on July 28th, 2014

Source: NASA & Google Earth

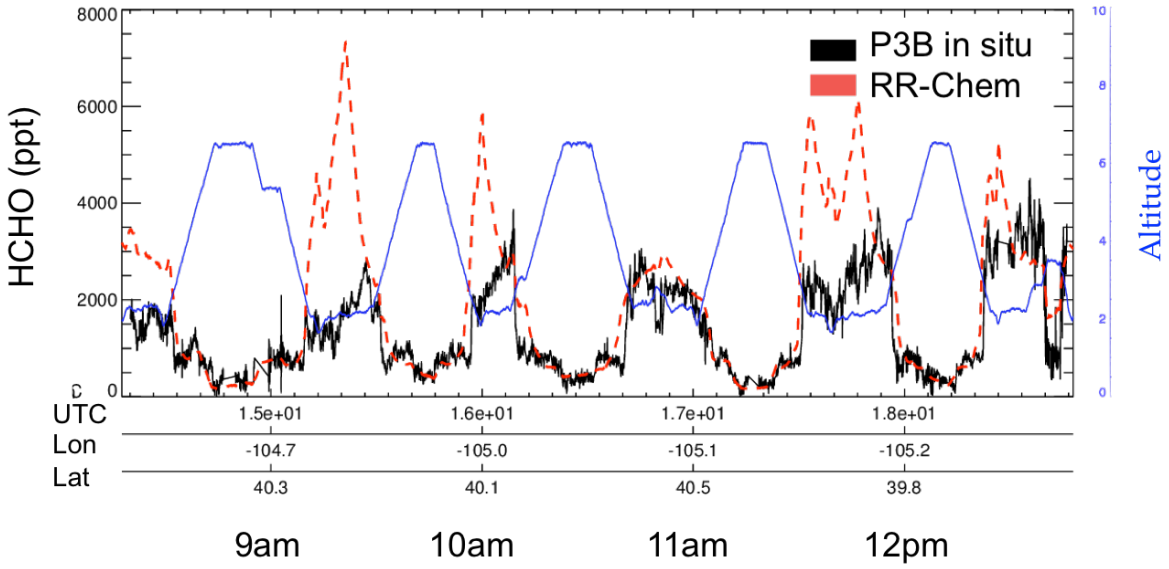

Figure 4.9: P3B in situ vs. RR-Chem HCHO (black, red) and altitude (blue) July 28th, 2014

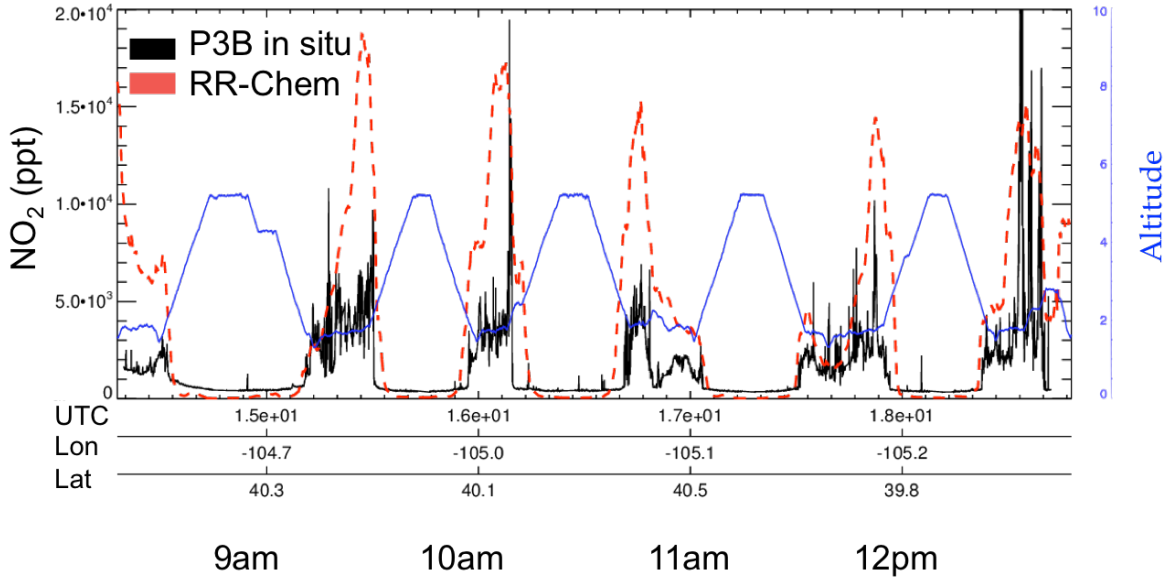

Figure 4.10: P3B in situ vs. RR-Chem NO_2 (black, red) and altitude (blue) July 28th, 2014

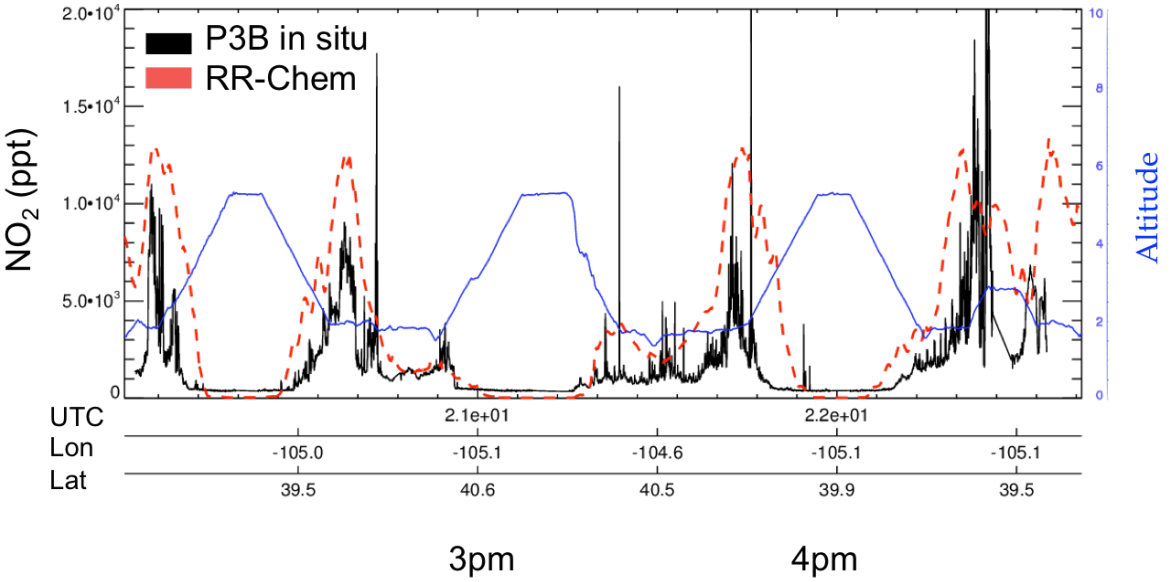

Figure 4.11: P3B in situ vs. RR-Chem NO_2 (black, red) and altitude (blue) July 28th, 2014

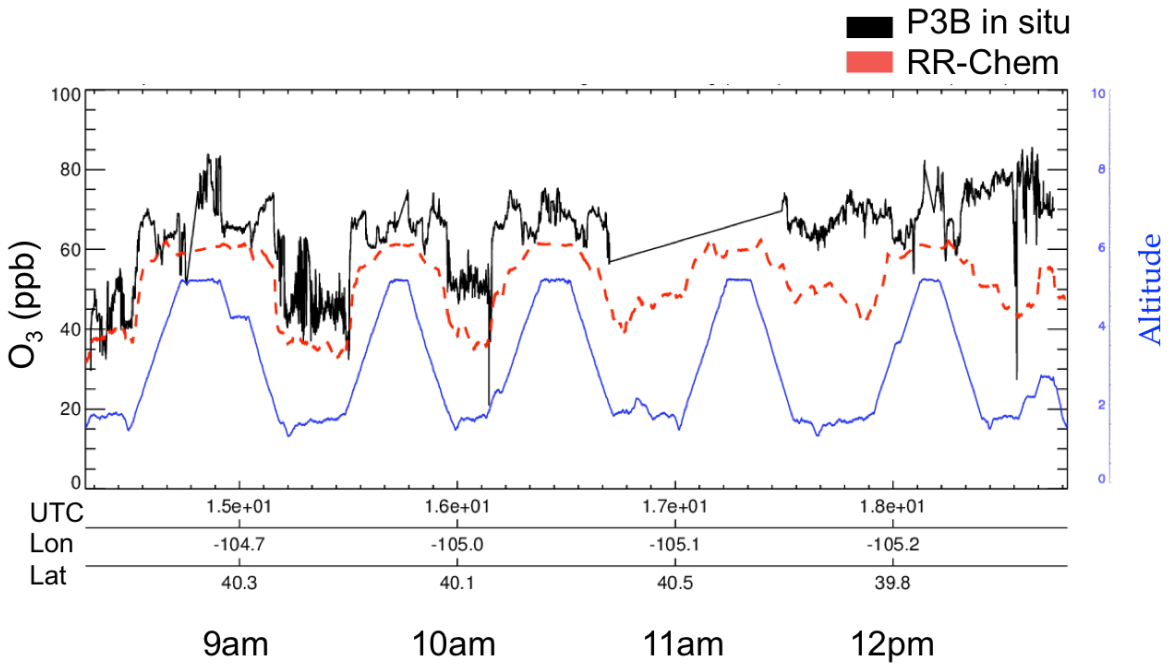

Figure 4.12: P3B in situ vs. RR-Chem O_3 (black, red) and altitude (blue)

July 28th, 2014

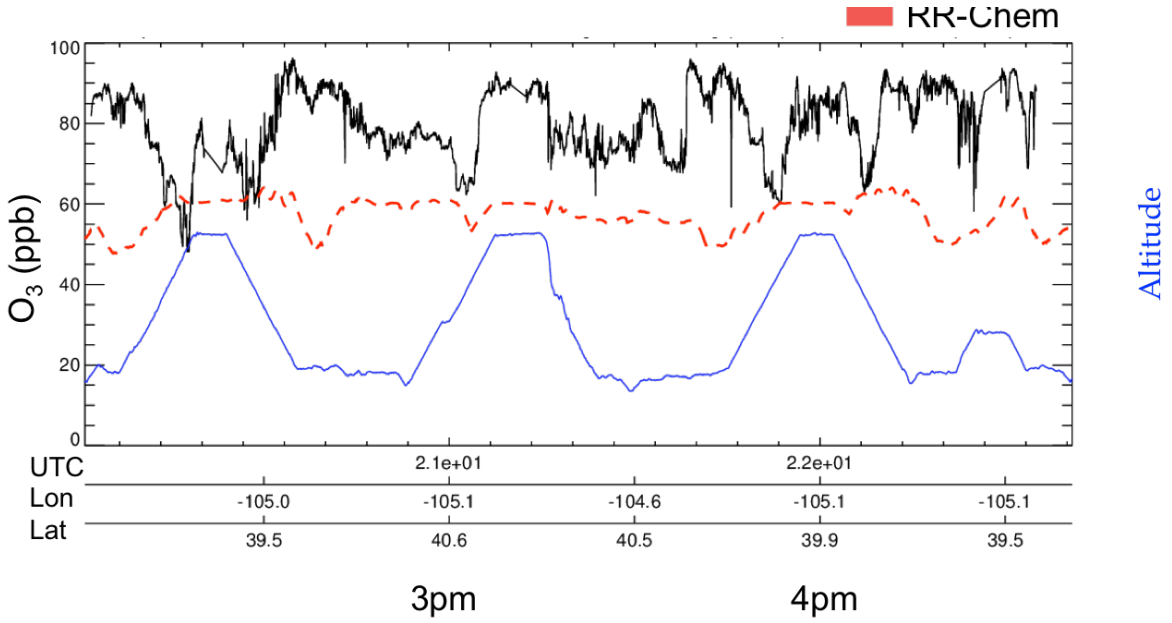

Figure 4.13: P3B in situ vs. RR-Chem O_3 (black, red) and altitude (blue)

July 28th, 2014

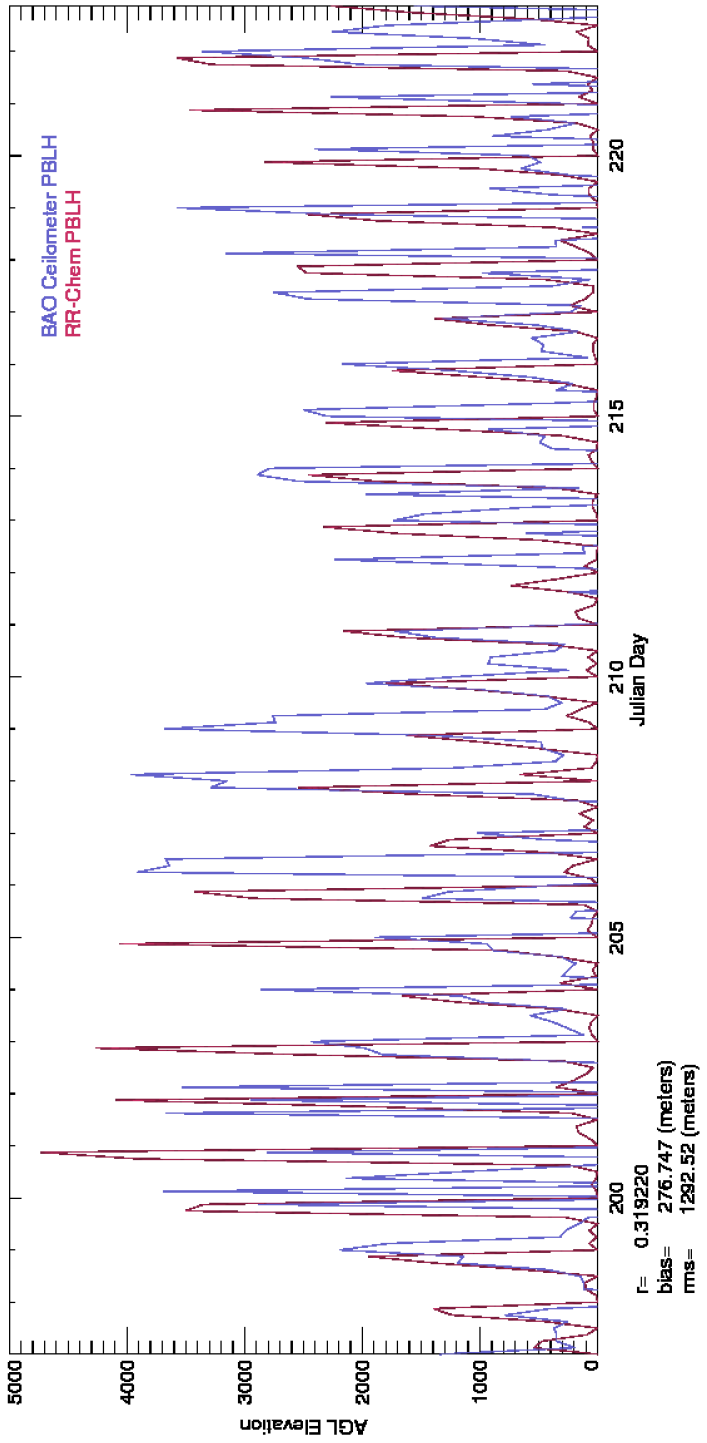

Figure 4.14: EPA Ceilometer vs. RR-Chem boundary layer height at BAO Tower

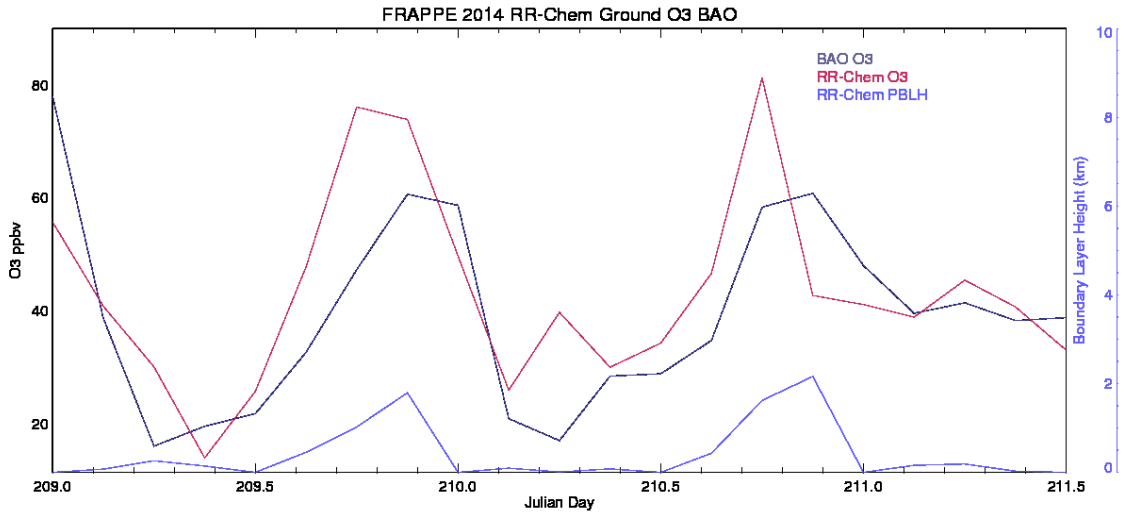

Figure 4.15: BAO measurements vs. RR-Chem O_3 (dark blue, red) and RR-Chem modeled boundary layer height (light blue)

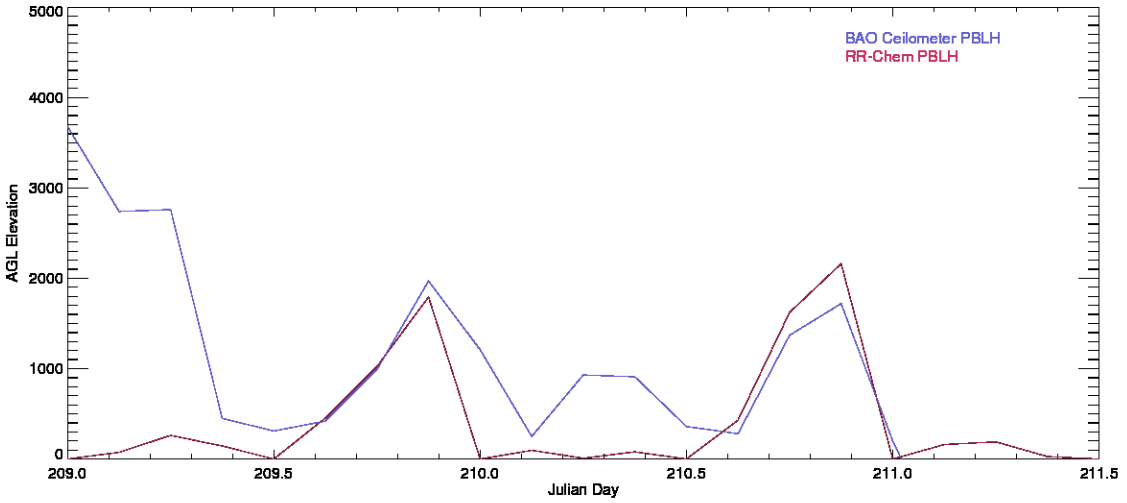

Figure 4.16: EPA Ceilometer measurements at vs. RR-Chem PBLH (blue, red) at BAO Tower

Chapter 4 References

Anderson, D. C., Loughner, C. P., Diskin, G., Weinheimer, A., Canty, T. P., Salawitch, R. J., … Dickerson, R. R. (2014). Measured and modeled CO and NOy in DISCOVER-AQ: An evaluation of emissions and chemistry over the eastern US. *Atmospheric Environment*, *96*, 78–87. doi:10.1016/j.atmosenv.2014.07.004

Barth, M. C., Wong, J., Bela, M. M., Pickering, K. E., Li, Y., & Cummings, K. (2014). Simulations of L ightning - Generated NOx for Parameterized C onvection in the WRF - Chem model, *4*(2), 15–20.

Charles, L. A., Chaw, S., Vladutescu, V., Wu, Y., Moshary, F., Gross, B., … Ahmed, S. (1970). Application Of CCNY Lidar And Ceilometers To The Study Of Aerosol Transport And PM2.5.

Czader, B. H., Li, X., & Rappenglueck, B. (2013). CMAQ modeling and analysis of radicals, radical precursors, and chemical transformations. *Journal of Geophysical Research: Atmospheres*, *118*(19), 11376–11387. doi:10.1002/jgrd.50807

EPA, (2013). 2011 National Emissions Inventory, Version 1 Technical Support Document, (November).

Ghude, S. D., Pfister, G. G., Jena, C., Van Der A, R. J., Emmons, L. K., & Kumar, R. (2013). Satellite constraints of nitrogen oxide (NOx) emissions from India based on OMI observations and WRF-Chem simulations. *Geophysical Research Letters*, *40*(2), 423–428. doi:10.1029/2012GL053926

Gross, B. M., Gan, C., Wu, Y., Moshary, F., & Ahmed, S. (n.d.). Remote sensing to improve air quality forecasts, 2–4.

Valin, L. C., Russell, a. R., Hudman, R. C., & Cohen, R. C. (2011). Effects of model resolution on the interpretation of satellite NO2 observations. *Atmospheric Chemistry and Physics*, *11*(22), 11647–11655. doi:10.5194/acp-11-11647-2011

Chapter 5: Conclusions

The primary task of chemical forecast modeling assessment is to understand how well the model works and what can be done to improve it. In general, RR-Chem performed satisfactorily and comparably to past studies in terms of ozone concentrations. Despite accurate modeling of ozone, the analysis of nitrogen dioxide and formaldehyde point to the fact that the model may be correctly predicting ozone for the wrong reasons. In addition, the high ozone concentrations observed on July 28th and 29th were not captured by the model leading to questions on the model's accuracy in simulating the Denver Cyclone and ability to capture urban chemistry.

For *in situ* measurements of methane, the model did not capture concentration enhancement near the surface. This problem is due to the neglect of anthropogenic sources of methane. Future model runs, especially for the Front Range where oil and natural gas development and production is rapidly expanding, need to include these sources. Likewise, carbon monoxide also was observed to have significant spikes near the surface, observed by the P3B and C130, which were not captured to the same degree by the model. Unlike methane, anthropogenic sources were included but the model still

underestimated observed concentrations most likely due to the coarse horizontal resolution.

Modeled formaldehyde saw a contrasting bias than that observed of methane and carbon dioxide. Formaldehyde was modeled with greater enhancement near the surface than what was observed *in situ* measurements. This was apparent not only in the general aircraft statistics but also in the case study. One limitation of this study was the comprehensiveness of volatile organic compound analysis. Formaldehyde was the only representative for VOC performance so future studies should seek to include a wider variety of volatile organic compounds. The complex nature of VOC emissions in the Front Range, particularly from the developing oil and natural gas industry, warrants further investigation and model analysis.

Nitrogen dioxide performance in RR-Chem had the highest bias of any of the variables analyzed. The model overpredicted by nearly three times the observed concentrations on average. Past studies have attributed the bias to the National Emissions Inventory's handling of mobile emissions in urban environments (Anderson et al., 2014; Chen et al., 2013). Despite this, the bias we found was significantly higher than previous studies, many that used the NEI 2005 and 2008 databases, leading to further questions of whether this is due to the NEI 2011 database bias or a model bias (EPA, 2013). Indeed

Anderson (2014) hypothesized the CO to NO_x ratios in the 2011 NEI database would contribute to a greater bias than their findings using the NEI 2008 database. Our analysis of OMI tropospheric NO2 column throughout the United States substantiate those previous works with very high model bias in urban environments and slight underprediction in the more rural areas. Nitrogen dioxides ability to decrease ozone concentrations, at relatively high amounts compared to local VOC concentrations, point to the model generally correctly predicting ozone for the wrong reasons. This in addition to other model physics, may have contributed to the lower than observed ozone concentrations during the case study.

The case study highlighted deficiencies in the model predictions during high ozone events coupled with the manifestation of unique dynamic features in the Front Range of Colorado. Modeled ozone was significantly underpredicted during the two-day ozone event that was analyzed, an atypical bias considering the generally good AirNow and RR-Chem comparison. This bias was hypothesized to be due to the model's inability to correctly model pollution concentrations within the Denver Cyclone in addition to other dynamics that acted on spatial scales smaller than the model's horizontal resolution. The boundary layer was investigated both generally and more intensely during the case study time period. The model's parameterized boundary layer was found to

capture the observed diurnal variations with little bias and temporal lag. The slight temporal lag of the boundary may have contributed to incorrect atmospheric pollutant concentrations in the late morning and early afternoon during the case study. That being said, the boundary layer was both over and underpredicted by the model during the case studying ruling it out as the source of the errors in modeled concentrations of ozone during this time period.

The rapid population growth of the Front Range coupled with unique dynamic flows and emissions merit further investigation and study of the area. Despite the several deficiencies of the model, more accurate emission inventories and a higher resolution model grid should greatly improve model accuracy. The critical focus of model improvement should be working with the National Emissions Inventory to conduct further assessment in improving nitrogen oxide emissions that contribute to not only NO_2 concentration inaccuracies but also ozone concentration inaccuracies. The importance of field missions like FRAPPE and DISCOVER-AQ has been highlighted, as they are crucial in chemical forecast model assessment. One possible solution in monitoring atmospheric pollutant concentrations on a more regular basis could be to deploy drones that would not only save money but also generate more continuous vertical measurements for model comparison (Basly et al., 2010).

Chapter 5 References

Anderson, D. C., Loughner, C. P., Diskin, G., Weinheimer, A., Canty, T. P., Salawitch, R. J., … Dickerson, R. R. (2014). Measured and modeled CO and NOy in DISCOVER-AQ: An evaluation of emissions and chemistry over the eastern US. Atmospheric Environment, 96, 78–87. doi:10.1016/j.atmosenv.2014.07.004

Basly, L., Wald, L., Basly, L., Wald, L., Laurini, R., Second, T., … Antipolis, S. (2010). Remote sensing and air quality in urban areas To cite this version : Remote Sensing and Air Quality in Urban Areas, (May 2000).

Chen, D., Li, Q., Stutz, J., Mao, Y., Zhang, L., Pikelnaya, O., … Pollack, I. B. (2013). WRF-Chem simulation of NOx and O3 in the L.A. basin during CalNex-2010. Atmospheric Environment, 81(x), 421–432. doi:10.1016/j.atmosenv.2013.08.064

EPA. (2013). 2011 National Emissions Inventory, Version 1 Technical Support Document, (November).